

BEXYL
BEYOND XYLELLA

Analysis of ecological impacts associated with *Xylella fastidiosa* outbreaks and disease management measures

Deliverable 8.3

20 August 2025

Author(s): Pablo Gonzalez-Moreno, Ricardo Enrique Hernández-Lambraño, María Fernández-Bravo, Francisco José Ruiz-Gómez, Rocío Hernandez-Clemente and Enrique Quesada-Moraga (P3-UCO); Montserrat Vilà (P1-CSIC-EBD); Concepción Olivares, Giovana P. F. Macan, Guillermo León-Ropero, Juan A. Navas-Cortés and Blanca B. Landa (P1-CSIC-IAS)

Funded by the European Union

DELIVERABLE INFORMATION

Start of the project:	01 Sep 2022
Duration:	48 months
Coordinator:	Blanca B. Landa
Deliverable title: Analysis of ecological impacts associated with Xf outbreaks and disease management measures	
Deliverable n°:	8.3
Nature of the deliverable:	Report
Dissemination level:	Public
WP contributing:	WP8
Lead beneficiary:	FCRA
Due date of deliverable:	31 Aug 2025
Actual submission date:	20 Aug 2025

Deliverable status

Ver.	Status	Date	Author(s)
1.0	Final	20 Aug 2025	Pablo Gonzalez-Moreno, Ricardo Enrique Hernández-Lambraño, María Fernández-Bravo, Francisco José Ruiz-Gómez, Rocío Hernandez-Clemente and Enrique Quesada-Moraga (P3-UCO); Montserrat Vilà (P1-CSIC-EBD); Concepción Olivares, Giovana P.F. Macan, Guillermo León-Ropero, Juan A. Navas-Cortés and Blanca B. Landa (P1-CSIC-IAS)

Disclaimer

The content of this deliverable does not necessarily reflect the official opinions of the European Commission or other institutions of the European Union.

Funded by the European Union

Content

1. **General introduction** 4
2. **Influence of environmental factors on the impact of *Xylella fastidiosa* on the phytosanitary conditions of almond trees and surrounding natural vegetation** 6
2.1 Materials and methods *6*
2.1.1 Study area 6
2.1.2 Field surveys 7
2.1.3 Plant DNA extraction and molecular detection of *Xf* 7
2.1.4 Environmental variables 8
2.1.5 Species diversity indexes 9
2.1.6 Data analyses 9
2.2 Results *9*
2.1.1. Phytosanitary status of surveyed orchards and natural vegetation 9
2.1.2. Models of defoliation and dead branch on almond orchards 10
2.1.3. Models of discoloration and dead branch on the surrounding nat. vegetation 13
3. **Impact of *Xylella fastidiosa* infection on Arthropod vectors distribution** 14
3.1. Materials and methods *15*
3.1.1. Arthropod Sampling Procedure 15
3.1.2. Taxonomic Identification 15
3.2. Results *16*
4. **Effect of *Xylella fastidiosa* infections and almond tree eradication on soil quality of almond orchards** 20
4.1. Materials and methods *20*
4.1.1. Soil sampling 20
4.1.2. Soil physicochemical analysis 22
4.1.3. Bacterial Population Densities 22
4.1.4. Isothermal microcalorimetry analysis 23
4.1.5. Bacterial Community level physiological profiles 23
4.1.6. Statistical analysis 24
4.2 Results *24*
4.2.1 Soil physicochemical analysis 24
4.2.2 Bacterial Population Densities 26
4.2.3 Isothermal microcalorimetry analysis 27
4.2.4 Bacterial Community level physiological profiles 33
5. **General conclusions** 35
6. **References** 36

Funded by the European Union

1. GENERAL INTRODUCTION

Freedom of movement and transport of goods, land abandonment, and climatic change are factors associated with global change and often linked to the emergence and invasion of plant pathogens (Gilbert and Parker, 2023). Within this context, the emergence and spread of plant pathogens have become a significant concern (Johnson et al., 2015). Invasive plant pathogens can exert a considerable influence on both natural and agricultural systems, affecting biodiversity, crop yield, landscape structure, and ecosystem functioning (Mordecai, 2011). While the impact of plant pathogens on agricultural systems has received high research attention, there has been remarkably little effort to investigate their effects at the forest-agriculture interface (Alexander et al., 2014). Forest-agriculture interfaces are widely recognized for providing services such as biodiversity reservoirs and controlling pests through natural mechanisms (Decocq et al., 2016). For instance, plant pathogens can exploit the interconnectedness between natural and agronomic systems (Gilbert, 2002), to favour their growth and spread through alternate or alternative wild hosts (Ristaino et al., 2021). Additionally, pathogen spread dynamics at the agroecological interfaces can be modulated by stressful environmental conditions (Burdon and Zhan, 2020). Thus, to develop better management strategies to minimize the adverse effects of invasive plant pathogens, it is needed to empirically investigate plant health in the forest-agriculture interface across environmental gradients (Singh et al., 2023).

Xylella fastidiosa (*Xf* hereafter) stands out among the invasive plant pathogens posing a major threat to global food security and plant biodiversity (Wells et al., 1987). In Europe, it has emerged as a top quarantine pathogen due to its extensive genetic variability and a wide range of plant hosts (Schneider et al., 2021), affecting economically important crops such as grapevines, citrus, olive and almond trees (De la Fuente et al., 2024). First identified during a severe outbreak in olive trees in Italy in 2013 (Sicard et al., 2018) *Xf* has recently caused outbreaks in France, Portugal, and Spain (EFSA et al., 2025). In mainland Spain, it is mainly associated with almond decline in Alicante, with large-scale eradication efforts underway (GVA, 2024; Velasco Amo et al., 2025).

Most efforts to unravel the impacts of *Xf* have focused on determining the mechanisms by which this pathogen disrupts tree crop health (Greco et al., 2021), and those studies have focused on a limited number of crops (De la Fuente et al., 2024). However, there has been limited research on the positive and negative interaction with natural areas, where many host plants from the natural environment have been identified as *Xf* hosts which may play a fundamental role on epidemiology of *Xf*-associated diseases (De la Fuente et al., 2024). There is also scarce information on how recent outbreaks are modulated by the interaction of *Xf* with abiotic factors (e.g., climate and landscape characteristics), biotic factors (e.g., *Xf* host plants and plant diversity) and management practices.

Among abiotic factors, it is known that climate plays a significant role in infection and spread of plant pathogens. For instance, extreme weather events (droughts, heatwaves, floods) influence disease development, favour bacterial growth and spread (Pandey et al., 2017), and exacerbate crop stress making them more susceptible to the attack of insects and pathogens (Teshome et al., 2020). In terms of biotic factors, asymptomatic host plants in natural habitats can act as disease reservoirs, facilitating pathogen spread in forest-agriculture interfaces

Funded by the European Union

(Roossinck and García-Arenal, 2015). In contrast, the benefits of these interfaces on agriculture are widely recognized, such as being a biodiversity reservoir for pest control (Decocq et al., 2016). Overall, the intricated web of interactions between *Xf* and its host plant species both in agricultural and forest vegetation and the far-reaching consequences for biodiversity, remains largely unexplored and a challenge for *Xf* research (De la Fuente et al., 2024). *Xf* transmission depends on insect vectors. In Europe two main species, *Philaenus spumarius* L. and *Neophilaenus campestris* Fallen, have been identified feeding on xylem fluid for plant-to-plant transmission from a large number of plant species (Cornara et al., 2019). Therefore, it is complicate to establish a hypothesis on how plant diversity of adjacent forest habitat can affect the incidence of *Xf* in nearby almond orchards. This positive or negative relationship will vary depending on factors acting simultaneously, such as plant community composition, microclimate, or crop management. For instance, shrub encroachment into orchards can reinforce the disease burden by acting as reservoirs for pathogens (Johnson et al., 2015). Moreover, shrubs can exacerbate infection by providing shelter and breeding sites for insect vectors, thereby serving as potential sources of pathogen inoculum (Cornara et al., 2019). Finally, the reduction in integrated pest management practices also contributes to increased disease pressure by failing to effectively secure plant hosts for pest control. Therefore, understanding the interaction of *Xf* with abiotic, biotic and management factors could provide valuable information to predict future changes in the health of both agricultural and forest ecosystems.

In addition to the ecological and epidemiological effects of *Xf* outbreaks, eradication measures implemented to control the disease can also have significant consequences for soil quality in affected orchards. In the case of almond groves, the enforced removal of infected trees and the subsequent abandonment of cultivated land may lead to changes in key soil parameters, including nutrient availability, microbial activity, and organic matter dynamics. Moreover, the incorporation of chipped woody material into the soil—a common practice following eradication—can alter soil microbial communities and affect decomposition processes, with potential long-term effects on soil structure and fertility. The presence of infected trees before removal may also influence soil properties through shifts in rhizosphere activity, nutrient cycling, and the release of stress-related compounds. Despite its importance, the impact of disease outbreaks and eradication strategies on soil quality remains poorly understood and deserves further investigation, particularly within the broader context of agroecosystem sustainability and land recovery.

Funded by the European Union

2. INFLUENCE OF ENVIRONMENTAL FACTORS ON THE IMPACT OF *XYLELLA FASTIDIOSA* ON THE PHYTOSANITARY CONDITIONS OF ALMOND TREES AND SURROUNDING NATURAL VEGETATION

We addressed the influence of *Xf* presence and its interaction with environmental drivers on the phytosanitary status (as measured by general decline and desiccation symptoms associated to *Xf* infection) of almond orchards and their surrounding natural vegetation in Alicante (Spain). Our specific aims were: i) to characterize the prevalence of *Xf* in orchards and in the surrounding vegetation in a forest-agriculture interface in the DA of Alicante, Spain; ii) to analyse the relationships between the *Xf* prevalence and the environmental drivers (climate, topography, landscape features and plant diversity) and crop management, and iii) to determine whether the plant diversity at the forest-agriculture interface could act as *Xf* reservoir or as a buffer, reducing the negative effects of the pathogen in the crop. We hypothesized that higher plant diversity would mitigate *Xf*-related damage by limiting pathogen transmission, while environmental stressors, particularly drought, and landscape fragmentation, would amplify disease severity in almond orchards.

2.1 Materials and methods

2.1.1 Study area

The study was conducted in the demarcated area (DA) of Alicante, Spain, affected by *X. fastidiosa* subsp. multiplex ST6 (Velasco Amo et al., 2025) (**Figure 1**). The region has a semi-arid Mediterranean climate with mean annual temperatures around 18 °C and low precipitation (290–460 mm/year) (Valdes-Abellan et al., 2017). Summers are hot and dry, winters mild (Kelley et al., 2012). The landscape consists of cretaceous limestone and marls, ranging from sea level to 1400 m (Alfaro García et al., 2004), and includes drought-adapted vegetation across cultivated areas, pine forests, and coastal zones (Duguy and Vallejo, 2008; Valdes-Abellan et al., 2017).

Funded by the European Union

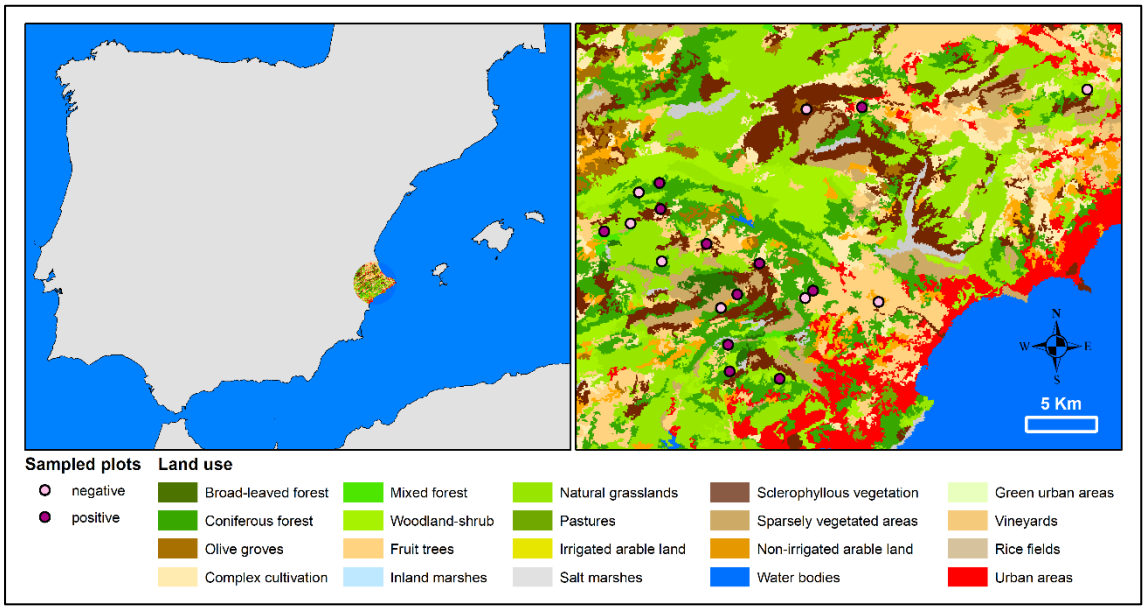


***Figure 1**: Distribution of sampled plots and land uses in the study area with indication of the positive and negative Xf infected plots sampled in this study.*

2.1.2 Field surveys

Field surveys were conducted in June–July 2023 across 19 almond orchards at the forest-agriculture interface, selected along a gradient of *Xf* prevalence and environmental conditions. Orchards were paired (positive/negative for *Xf*; **Figure 1**) based on preliminary data from the regional monitoring network (GVA, 2024). In each plot, six almond trees were visually assessed for symptoms (defoliation and dead branches) using a 0–100% scale (Eichhorn et al., 2016), and shrub cover estimated at their base. Plant diversity in adjacent vegetation was recorded along two 50 m transects, noting species identity, distance to the orchard edge, and symptoms (discoloration and dead branches) using a 0–100% scale (Eichhorn et al., 2016).

2.1.3 Plant DNA extraction and molecular detection of *Xf*

For *Xf* diagnosis, samples of mature branches and leaves from almond trees and surrounding vegetation were collected following EPPO protocol PM7/24 (EPPO, 2023). High-prevalence host species (GVA, 2024) were targeted, selecting symptomatic individuals up to 50 m from orchard edges. DNA was extracted using the CTAB method, with controls included. *Xf* detection was performed via duplex qPCR (Bonants et al., 2019), modifying the EPPO protocol with iTaq™ Supermix and BSA to prevent PCR inhibition. Cq values ≤35 were positive, >38 negative, and 35–38 inconclusive, requiring retesting (EPPO, 2023). Positive controls ensured consistency across runs.

Funded by the European Union

2.1.4 Environmental variables

Climatic, topographic and landscape features of the plots were obtained from public repositories (**Table 1**). Climatic data (annual and seasonal values of temperature, precipitation and evapotranspiration) were downloaded from CHELSA (http://chelsa-climate.org/) a 30 arc-second resolution (~900 m). We calculated Compound Topographic Index (CTI) and Heat load index (HLI) (Evans et al., 2014), from a Digital Elevation Model (DEM) by National Center for Geographic Information of Spain at 5 m spatial resolution (CNIG Spanish acronym; http://centrodedescargas.cnig.es).

Because of its effect on pathogen dispersion, we included some Landscape metrics to describe aspects of the landscape configuration and composition: the total area of forest (Lforest), total area of shrublands (Lshrub), and connexion index (CONTAG). Metrics were assessed in a circular area of 1000 m radii around the 19 plots selected using Spanish Land Use and Land Cover Information System map (SIOSE AR; http://centrodedescargas.cnig.es), and metrics were calculated using the "landscapemetrics" package (Hesselbarth et al., 2019), in R (R Core Team, 2019).

***Table 1**: Variables used as predictors of the* Xf *impact both in almond crops and adjacent natural vegetation.*

Variables	Description	Source	Range
pet_mean	Annual mean of potential transpiration (kg m-2 month-1)	CHELSA (http://chelsa-climate.org/)	0.92–1.15
pet_range	Annual range of potential transpiration (kg m-2 month-1)		1.25–1.46
bio1	Mean annual air temperature (ºC)		11.85–17.95
bio12	Annual precipitation amount (kg m-2)		574.2–822.9
bio15	Precipitation seasonality (CV)		45.1–48.9
cti	Compound Topographic Index	DEM (http://centrodedescargas.cnig.es)	8.54–10.42
hli	Heat load index		0.75–0.85
Lshrub	Total area of shrub landscape (ha)	SIOSE AR (http://centrodedescargas.cnig.es)	26.46–255.78
***Xf* almond**	Presence of *Xylella fastidiosa* in almond trees	Field campaign	0–1
***Xf* host**	Presence of *X. fastidiosa* in surrounding host plant species		0–1
***Xf* plot**	Presence of *X. fastidiosa* in sampled plots		
Lforest	Total area of forest landscape (ha)		0–203.84
contag	Landscape connexion index		31.74–65.87
Cshrub	Percentage of vegetation cover in the orchards (%)		0–100
H	Shannon diversity index of the surrounding natural vegetation		1.99–3.22
H_spPrev	Shannon diversity index of the *Xf* host plant species in surrounding natural vegetation		0–1.96
abundance_spPrev	Abundance of the *Xf* host plant species in surrounding natural vegetation (*n*)		4–278

Funded by the European Union

2.1.5 Species diversity indexes

To quantify plant diversity at the surrounding natural vegetation per plot, we calculated the following indices: Species abundances and the Shannon diversity index (H). H was calculated using the function diversity of the "Vegan" package (Oksanen et al., 2022) in R.

2.1.6 Data analyses

We used Generalized Linear Mixed Models (GLMMs) within a multimodel inference framework (Burnham and Anderson, 2002), to assess the impact of *Xf* presence and environmental factors on almond tree and surrounding *Xf* host plant health. Response variables included defoliation and dead branches in almond trees and discoloration and dead branches in surrounding *Xf* host plant. Models assumed a log-normal error distribution, included "plot ID" as a random effect, and were fitted using Gaussian quadrature approximation. Predictor variables were screened for collinearity (r ±0.7), selected based on biological relevance, and standardized (mean = 0, SD = 1). Model selection followed an all-subsets approach using Akaike's Information Criterion corrected (AICc), considering models within four AICc units of the best model (Hernández-Lambraño et al., 2018). Akaike weights (wi) were used to rank predictor importance, and regression coefficients were estimated as weighted averages across models (Burnham and Anderson, 2002). All statistical analyses were performed in R. The lme function of the "nlme" package was used to fit the linear mixed-effects models (Pinheiro et al., 2020) and the MuMIn package was used to perform the multi-model selection (Barton, 2022).

2.2 Results

2.1.1. Phytosanitary status of surveyed orchards and natural vegetation

Across the 19 surveyed plots, qPCR confirmed the presence of *Xf* in 36 of the 114 almond trees sampled. Among the plots initially selected as non-infected, two presented at least one tree with positive identification of *Xf*. Conversely, two plots previously diagnosed as positive, did not exhibit any *Xf*-positive almond tree after qPCR analysis. After these results, positive and negative plots were assigned based on current results. Defoliation and dead branch rates of almond trees in plots varied between 11.6 ± 11.2 to 71.6 ± 15 and from 1.66 ± 2.58 to 57.5 ± 25.6 (% mean±SD), respectively. Defoliation and dead branch exhibited a significant increase in trees infected with *Xf* compared to the non-infected trees ($t = -5.07$, $p < 0.001$ and $t = -2.61$, $p = 0.01$, respectively).

Regarding the 353 samples collected from various host plant species in the surrounding vegetation, 155 or 154 were sampled around the *Xf*-non-infected or *Xf*-infected almond plots, respectively. In total, 22 plant species were sampled in the 19 surveyed plots, with 15 species being present in both types of almond orchards (**Table 2**). A total of 40 (11.4%) of all sampled plants tested positive for *Xf* by qPCR. The species with the highest incidence of positive plants in both type of orchards were *Ulex parviflorus* (37.5%), *Rhamnus alaternus* (17.5%), *Cistus albidus* (15%), and *Salvia rosmarinus* (12.5%); the three formers being found infected in both types of orchards. Notably, 87.5% of the 40 *Xf*-positive samples were obtained from areas

Funded by the European Union

adjacent to almond orchards infected by *Xf*, with the highest number of positive samples from *Calicotome spinosa* (5.0%), *C. albidus* (12.5%), *Cistus salviifolius* (5.0%), *R. alaternus* (15.0%), *S. rosmarinus* (12.5%), and *U. parviflorus* (32.5%). Conversely, only 12.5% of all positive samples came from areas not surrounded by *Xf*-infected almond orchards. In these cases, *C. albidus* (2.5%), *R. alaternus* (2.5*%), Santolina chamaecyparissus* (2.5%), and *U. parviflorus* (5.0%) were the only infected species among the 15 analysed (**Table 2**).

Cq values obtained by the Ouyang-qPCR test were lower than those of Harper-qPCR tests; consequently, only those of the later were considered (data not shown). In general, the Cq values of qPCR were lower for the samples obtained surrounding the *Xf*-infected almond plots (16.3 to 38.0) with a few exceptions indicating a higher inoculum concentration of the bacterium as compared to Cq values obtained for the plants sampled in areas surrounding non-infected almond orchards (32.7 to 36.3) (**Table 2**). Two samples, one from *Bupleurum fruticescens* and the other from *R. lycioides*, exhibited Ct values close to the detection limit (38.2 and 36.0) with some inconclusive results when repeated. Due to the destructive sampling no additional plant material was left for confirmation. If those plant species are sampled again and confirmed positive through qPCR by the (GVA, 2024), these species will be considered new host plants for *Xf* at the Alicante DA (**Table 2**).

Discoloration rates of host plant species in surrounding natural vegetation did not significantly differ between *Xf*-infected and non-infected individuals ($t = -1.72$, $p = 0.09$). Similarly, dead branch rates showed no significant variation between groups ($t = -1.21$, $p = 0.22$).

2.1.2. Models of defoliation and dead branch on almond orchards

Leaf defoliation and the percentage of dead branches of almond trees were correlated with shrub cover, *Xf* presence, abundance of *Xf* host species, landscape configuration and climate factors, albeit not with the presence of *Xf* in surrounding host plant species **(Table 3, Table 4**). Specifically, leaf defoliation and the percentage of dead branches were positively correlated with shrub cover in orchards and *Xf* presence. Almond tree defoliation increased positively with higher abundance of *Xf* host plant species in the surrounding vegetation, and in areas with higher seasonal evapotranspiration; in contrast, it decreased with landscape connexion index and diversity of *Xf* host species. Dead branch rates in almond trees were negatively related to potential evapotranspiration.

Funded by the European Union

Table 2: *Host plant species sampled in the natural vegetation surrounding the* Xylella fastidiosa *infection status of almond orchards*

X. fastidiosa infection status	Host plant	qPCR (analysis)[a]			Plants analysed (N)
		Negative	Positive	(Cq value)	
Negative	*Asparagus acutifolius*	3	0		3
	Calicotome spinosa	14	0		14
	Cistus albidus	17	1	(35.7)	18
	Cistus salviifolius	4	0		4
	Helichrysum italicum	14	0		14
	Helichrysum stoechas	8	0		8
	Lavandula latifolia	10	0		10
	Olea europaea	6	0		6
	Phagnalon saxatile	10	0		10
	Rhamnus alaternus	16	1	(35.1)	17
	Rhamnus lycioides	5	0		5
	Salvia rosmarinus	19	0		19
	Santolina chamaecyparissus	8	1	(36.3)	9
	Staehelina dubia	3	0		3
	Ulex parviflorus	19	2	(33.5-35.9)	21
	Unknown	1	0		1
	Sub-Total	155	5	(32.7-36.3)	162
Positive	*Asparagus acutifolius*	3	0		3
	Bupleurum frutiscescens	0	1	(38.2)	1
	Calicotome spinosa	9	2	(22.9-35.6)	11
	Cistus albidus	18	5	(25.5-35.2)	23
	Cistus salviifolius	2	2	(25.0-34.6)	4
	Coronilla juncea	1	0		1
	Fumana ericoides	2	0		2
	Helichrysum italicum	20	0		20
	Helichrysum stoechas	7	0		7
	Lavandula latifolia	4	0		4
	Medicago sativa	2	0		2
	Olea europaea	6	0		6
	Osyris alba	1	0		1
	Phagnalon saxatile	8	0		8
	Quercus coccifera	3	0		3
	Rhamnus alaternus	24	6	(30.5-36.6)	30
	Rhamnus lycioides	2	1	(36.0)	3
	Salvia rosmarinus	19	5	(19.4-37.0)	24
	Santolina chamaecyparissus	14	0		14
	Staehelina dubia	3	0		3
	Ulex parviflorus	8	13	(16.3-38.0)	21
	Sub-Total	154	35	(16.3-38.0)	191
	Total	309	40	(16.3-38.0	353

[a] Samples were identified to be infected by *Xf* using the qPCR test of (Bonants et al., 2019) that combined the protocols of (Harper et al., 2010) and (Ouyang et al., 2013). Only data from the qPCR-harper were considered.

Funded by the European Union

We found significant interactions between the *Xf* infected orchards and seasonal evapotranspiration (β = 0.03 ± 0.008, p < 0.001), landscape with shrub cover (β = 0.24 ± 0.009, p < 0.001), abundance of *Xf* host species (β = 0.15 ± 0.009 p < 0.001) and topographic wetness (β = -0.38 ± 0.008, p < 0.001). Specifically, *Xf* infected orchards showed more defoliation in orchards with higher seasonal evapotranspiration, landscape with higher shrub cover and higher abundance of host species, in comparison to non-infected orchards (**Figure 2**). Infected orchards localised in areas with less soil water retention capacity showed a significant tendency to increase defoliation compared to non-infected ones.

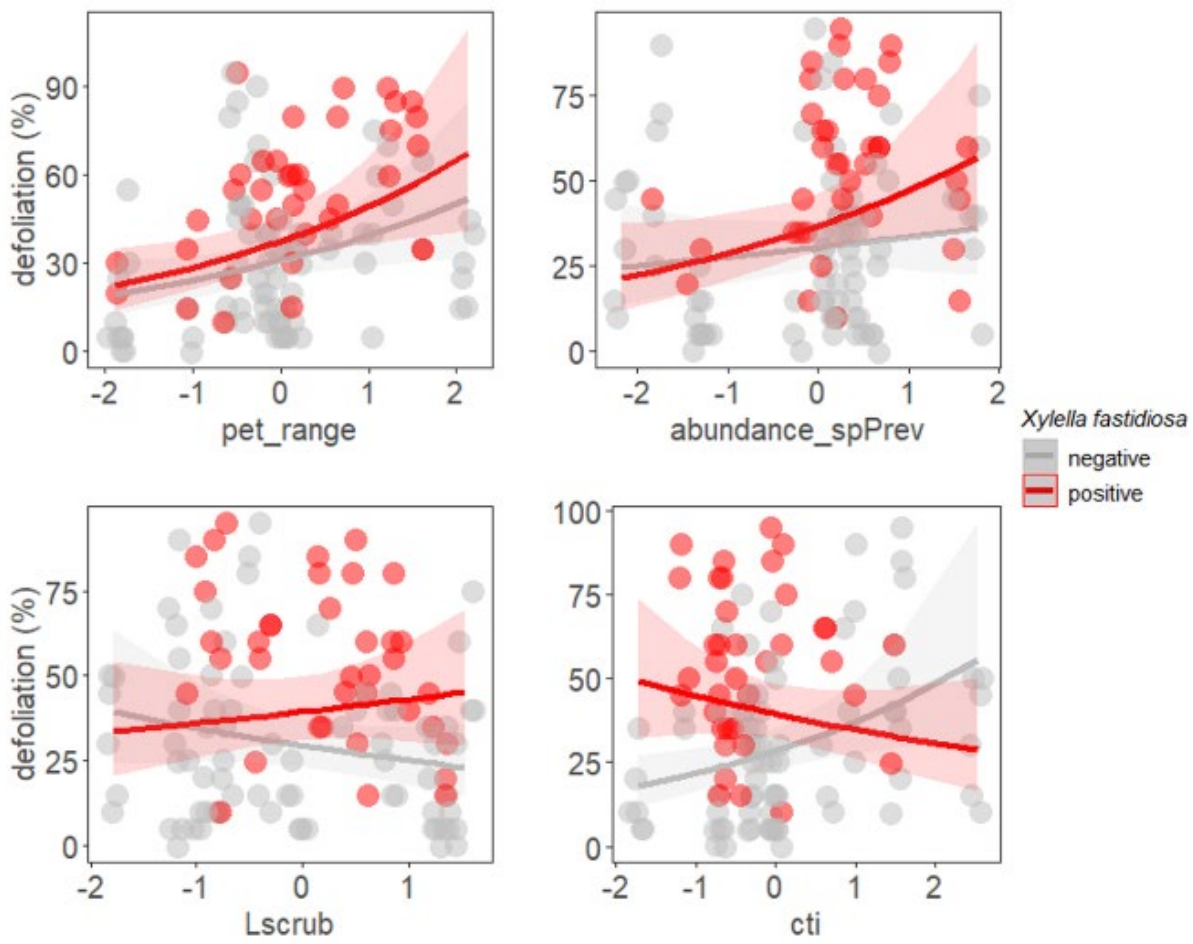


***Figure 2**: Defoliation levels in almond orchards related to seasonal evapotranspiration, abundance of Xf host plants, shrub landscape and compound topographic index. Red line and dots represent almond orchards infected with Xf, while grey line and dots correspond to almond orchards without Xf. Predictor variables were standardized (mean = 0, SD = 1) to allow for direct comparison of effect sizes.*

Funded by the European Union

2.1.3. Models of discoloration and dead branch on the surrounding natural vegetation

Leaf discoloration and the percentage of dead branches of *Xf* host plants in natural vegetation were correlated with plant species diversity, distance to crop edge, abundance of *Xf* host plant species, and climate factors, albeit not with the presence of *Xf* both in the orchards with natural vegetation and in the almond trees (**Table 5, Table 6**). Specifically, plant discoloration was higher in orchards with greater plant diversity and those located farther from the almond orchards. Additionally, an increased abundance of *Xf* host species and higher temperatures, coupled with lower precipitation levels, were associated with greater leaf discoloration. Finally, the percentage of dead branches in natural plant species increased in areas located far from the almond orchards.

***Table 3**: Multimodel inference results of the averaged best models explaining defoliation in almond trees (conditional average on models < 4 AICc). For each predictor we provide the estimated coefficient, standard and adjusted error, significance, and accumulated weights (importance). In bold significant variables. See variable explanation in Table 1.*

Variable	Estimate	Std. Error	Adjusted SE	z value	Pr(>|z|)	SumWeights	N.models
(Intercept)	3.53	0.18	0.18	18.7	< 0.001		
Cshrub	0.11	0.003	0.003	39.7	< 0.001	1	28
***Xf* almond positive**	0.22	0.006	0.006	38.6	< 0.001	1	28
pet_range	0.24	0.08	0.08	2.97	0.003	1	28
abundance_spPrev	0.25	0.09	0.09	2.67	0.007	0.96	26
contag	-0.25	0.09	0.09	2.67	0.007	0.93	25
H_spPrev	-0.24	0.09	0.09	2.51	0.01	0.91	23
cti	0.14	0.09	0.09	1.49	0.13	0.47	15
***Xf* host positive**	-0.30	0.21	0.22	1.40	0.16	0.42	13
pet_mean	-0.07	0.08	0.08	0.84	0.39	0.17	5
Lshrub	-0.02	0.13	0.13	0.18	0.85	0.13	5
H	0.03	0.07	0.07	0.45	0.64	0.12	4
Lforest	0.02	0.06	0.06	0.42	0.67	0.12	4

***Table 4**: Multimodel inference results of the averaged best models explaining % dead branch in almond orchards (conditional average on models < 4 AICc). For each predictor we provide the estimated coefficient, standard and adjusted error, significance, and accumulated weights (importance). In bold significant variables. See variable explanation in Table 1.*

Variable	Estimate	Std. Error	Adjusted SE	z value	Pr(>|z|)	SumWeights	N.models
(Intercept)	2.91	0.33	0.33	8.78	< 0.001		
***Xf* positive**	0.12	0.007	0.007	17.8	< 0.001	1	225
Cshrub	0.01	0.004	0.004	5.10	< 0.001	1	225
pet_mean	-0.48	0.19	0.20	2.42	0.01	0.9	197
Lforest	-0.31	0.16	0.16	1.86	0.06	0.63	126
H	-0.26	0.16	0.16	1.61	0.10	0.45	93
abundance_spPrev	-0.26	0.17	0.17	1.50	0.13	0.44	97
pet_range	0.27	0.19	0.19	1.41	0.15	0.41	102
cti	0.24	0.17	0.17	1.39	0.16	0.37	88
contag	-0.26	0.22	0.22	1.15	0.24	0.33	84
***Xf* host positive**	0.53	0.46	0.47	1.14	0.25	0.29	75
Lshrub	-0.07	0.30	0.30	0.23	0.81	0.22	58
H_spPrev	-0.11	0.22	0.22	0.50	0.61	0.18	53

Funded by the European Union

***Table 5**: Multimodel inference results of the averaged best models explaining % discoloration of Xf host plants in surrounding natural vegetation (conditional average on models < 4 AICc). For each predictor we provide the estimated coefficient, standard and adjusted error, significance, and accumulated weights (importance). In bold significant variables. See variable explanation in Table 1.*

Variable	Estimate	Std. Error	Adjusted SE	z value	Pr(>|z|)	SumWeights	N.models
(Intercept)	2.62	0.17	0.17	15.0	< 0.001		
distance to crop	0.05	0.001	0.001	39.5	< 0.001	1.0	76
H	0.17	0.07	0.07	2.39	0.01	1.0	72
abundance_spPrev	0.26	0.11	0.11	2.34	0.01	1.0	71
bio12	-0.29	0.13	0.13	2.12	0.03	1.0	70
bio1	0.35	0.13	0.13	2.66	0.008	0.9	70
cti	-0.12	0.07	0.08	1.52	0.12	0.5	38
***Xf* host positive**	-0.25	0.20	0.20	1.23	0.21	0.4	28
bio15	0.13	0.26	0.26	0.51	0.61	0.3	33
Lforest	0.06	0.07	0.07	0.86	0.38	0.3	22
***Xf* plot positive**	0.12	0.15	0.15	0.81	0.41	0.2	22
Lshrub	0.01	0.09	0.09	0.15	0.87	0.2	17
hli	-0.003	0.08	0.08	0.03	0.97	0.2	16

***Table 6**: Multimodel inference results of the averaged best models explaining % dead branch of Xf host plants in surrounding natural plants (conditional average on models < 4 AICc). For each predictor we provide the estimated coefficient, standard and adjusted error, significance, and accumulated weights (importance). In bold significant variables. See variable explanation in Table 1.*

Variable[a]	Estimate	Std. Error	Adjusted SE	z value	Pr(>|z|)	SumWeights	N.models
(Intercept)	2.98	0.27	0.27	10.8	**< 0.001**		
distance to crop	0.06	0.001	0.001	57.6	**< 0.001**	1	72
***Xf* host positive**	-0.43	0.25	0.25	1.68	0.09	0.60	39
bio1	0.15	0.11	0.11	1.29	0.19	0.40	29
cti	-0.12	0.12	0.12	1.04	0.29	0.35	29
abundance_spPrev	-0.09	0.11	0.11	0.83	0.40	0.27	23
Lshrub	-0.09	0.10	0.10	0.91	0.36	0.24	19
bio12	-0.07	0.10	0.10	0.70	0.48	0.21	18
H	-0.03	0.10	0.10	0.33	0.73	0.16	15
***Xf* plot positive**	0.01	0.20	0.20	0.06	0.95	0.15	15

3. IMPACT OF *XYLELLA FASTIDIOSA* INFECTION ON ARTHROPOD VECTORS DISTRIBUTION

Xf is a xylem-limited bacterium transmitted exclusively by xylem-sap feeding insects belonging to the order Hemiptera, suborder Cicadomorpha. The main groups involved in its transmission are the superfamilies Cicadoidea, Cercopoidea (spittlebugs and froghoppers), and Membracoidea, particularly the families Cicadellidae (subfamily Cicadellinae) and Aphrophoridae. These groups vary in distribution and diversity depending on the geographical region, and their relevance as vectors depends on multiple factors such as transmission efficiency, biology, and behaviour. In this section our aim was to characterize the abundance and distribution of potential insect vectors of *Xf* in almond crops and neighbouring vegetation and its relationship with *Xf* infection status.

Funded by the European Union

3.1. Materials and methods

3.1.1. Arthropod Sampling Procedure

Arthropod communities were collected during the summer of 2023 (June–July) using a battery-powered backpack insect suction sampler. Sampling was conducted in 19 almond (*Prunus dulcis*) orchard plots with different *X. fastidiosa* infection statuses, and in adjacent semi-natural vegetation (see study area and details in **section 2.1** and **Figure 1**). In each plot, two linear 50-meter transects were established in the surrounding vegetation of the orchards. Each transect was subdivided into two consecutive 25-meter segments, with one sample collected per segment, yielding four transect samples per plot. Within each orchard, six individual almond trees were selected, and a sample was taken from the base of each tree, targeting the vegetation and litter beneath the canopy. The suction sampler was used to sample for one minute under each tree. This provided six additional samples per plot. All material was transported in sealed plastic bags and frozen in-situ in the demarcated area to avoid potential bio-risk hazards. Samples were then processed in the lab to reduce plant debris and preserved in 70% ethanol for further analysis. Because the suction sampling during the dry summer months collected large amounts of plant debris, dried vegetation, and soil particles, it was not feasible to conduct a full DNA-based metabarcoding analysis on all arthropods present. Therefore, the study focused exclusively on Hemiptera, as this order includes several families known to act as vectors of *Xylella fastidiosa*. Hemipteran specimens were manually separated from debris under a stereomicroscope, grouped into morphotypes based on external characteristics, and classified by developmental stage (adult or nymph) for subsequent analyses.

3.1.2. Taxonomic Identification

All hemipteran specimens were identified to family level based on external morphological characters, using the following taxonomic literature:

- Della Giustina, W. (n.d.). *Homoptères Cicadellidae. Volume 3: Compléments*. Paris: INRA.
- Holzinger, W. E., Kammerlander, I., & Nickel, H. (2003). *The Auchenorrhyncha of Central Europe: Fulgoromorpha, Cicadomorpha excl. Cicadellidae (Vol. 1)*. Leiden: Brill.
- Kunz, G., Nickel, H., & Niedringhaus, R. (2011). *Fotoatlas der Zikaden Deutschlands. Photographic Atlas of the Planthoppers and Leafhoppers of Germany*. Weikersheim: Goecke & Evers.
- Ribaut, H. (1936). *Faune de France, Volume 31: Homoptères Auchénorhynques. I (Typhlocybidae)*. Paris: Paul Lechevalier et Fils.
- Ribaut, H. (1952). *Faune de France, Volume 57: Homoptères Auchénorhynques. II (Jassidae)*. Paris: Paul Lechevalier et Fils.
- Royal Entomological Society. (2013). *Handbooks for the Identification of British Insects*. London: Royal Entomological Society.

Funded by the European Union

Selected morphotypes are currently undergoing molecular identification using the COI (cytochrome oxidase subunit I) barcode gene to achieve species or at least genus-level resolution.

3.2. Results

A total of 607 hemipteran individuals were collected. The most abundant family was Cicadellidae (504 individuals), followed by Issidae (66). Additional families included Aphrophoridae (4), Delphacidae (2), Membracidae (2), and Psyllidae (2). Forty-seven specimens were identified as Hemiptera but could not be confidently assigned to a family yet.

To assess the potential presence of known *Xf* vectors, we focused on two key hemipteran families: Cicadellidae and Aphrophoridae. Although the family Cercopidae includes known vector species, no individuals from this group have been identified in our samples so far. However, ongoing molecular analyses may reveal their presence among the currently unclassified hemipteran specimens. **Figure 3** presents the distribution of Cicadellidae and Aphrophoridae across the different microhabitats (natural vegetation transects vs. almond trees) and infection statuses (infected vs. non-infected plots).

To determine whether Cicadellidae abundances differed significantly across habitats (almond trees vs. natural vegetation transects) and infection statuses (infected vs. non-infected plots), we performed a Kruskal–Wallis test using plot-level data. The analysis revealed no statistically significant differences among the four groups ($\chi^2 = 5.63$, $p = 0.13$). Pairwise comparisons with Mann–Whitney U tests similarly showed no significant differences ($P > 0.07$). However, transects in infected plots consistently exhibited the highest Cicadellidae counts and showed near-significant tendencies when compared to transects in non-infected plots ($P = 0.07$) and almond tree samples from infected plots ($P = 0.09$). These results suggest that, while visual patterns (Figure 3) indicate a higher Cicadellidae abundance in transects from infected plots, the differences are not statistically supported at the current morphotype taxonomic resolution. Further species-level identification through ongoing COI barcoding will allow more robust testing of whether specific Cicadellidae taxa preferentially associate with certain habitats or infection statuses.

Results indicated that Cicadellidae individuals were consistently detected across all sampling categories, with notably higher abundances in transects located in plots infected with the disease. This pattern may suggest a greater affinity of this group for natural vegetation, possibly due to higher plant diversity or microclimatic conditions favorable to their development. The elevated counts in infected plots could either reflect local differences in vegetation structure or indicate a potential association between certain Cicadellidae species and diseased plants. However, this remains speculative and requires confirmation through species-level identification.

Funded by the European Union

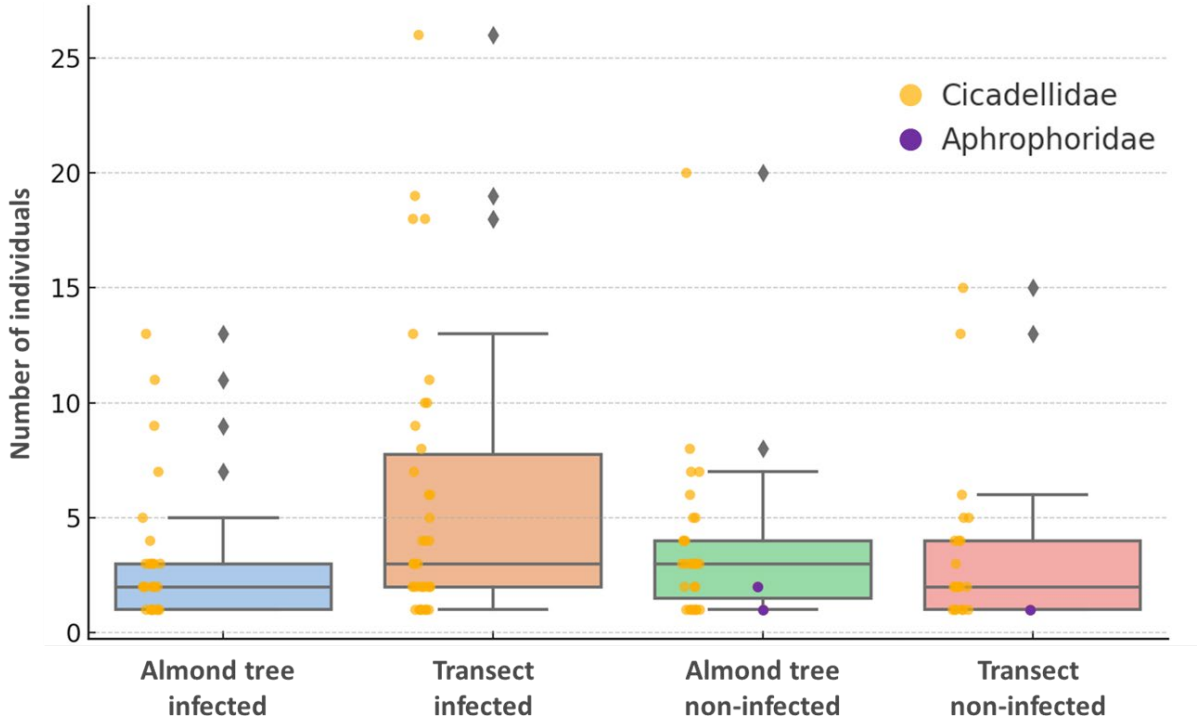


Figure 3: *Distribution of Cicadellidae (yellow) and Aphrophoridae (purple) individuals across all sampling units, grouped by habitat type (**almond** trees vs. natural vegetation **transects**) and **infection status** (infected vs. non-infected plots). Each point represents the number of individuals recorded in a single sampling unit. Boxplots indicate median, interquartile range, and outliers (grey diamonds).*

For Aphrophoridae, their extremely low and sporadic occurrence (only a few individuals across all samples) prevented meaningful statistical analysis. A Kruskal–Wallis test revealed no differences among groups ($\chi^2 \approx 0.2$, $P \approx 0.98$), which suggests that the rarity of this family in the collected samples is due to chance rather than the absence of ecological patterns. Given their recognized importance as vectors of *Xylella fastidiosa*, ongoing species-level identification will clarify whether these few individuals belong to vector-relevant taxa.

Our results indicated that Aphrophoridae were much rarer and detected only sporadically, which aligns with their known patchy distribution and seasonal population peaks. Although their numbers were low in our samples, this does not diminish their epidemiological relevance, as members of this family, such as *P. spumarius*, are recognized as primary vectors of Xylella fastidiosa in Europe.

To further explore the spatial distribution of potential vector groups, particularly Cicadellidae, we mapped the total number of individuals captured per plot, distinguishing between those collected from almond trees and natural vegetation transects (**Figure 4**). The heatmap reveals notable variability across sampling locations, with some infected plots (such as AL7 and AL6) showing markedly higher Cicadellidae abundance, especially in the transects. This pattern may reflect differences in vegetation structure, microclimatic conditions, or broader landscape features, all of which can influence vector density and movement. The greater numbers in transects of infected plots may point to a potential link between vegetation

Funded by the European Union

dynamics and disease presence, although this hypothesis remains to be tested with higher taxonomic resolution.

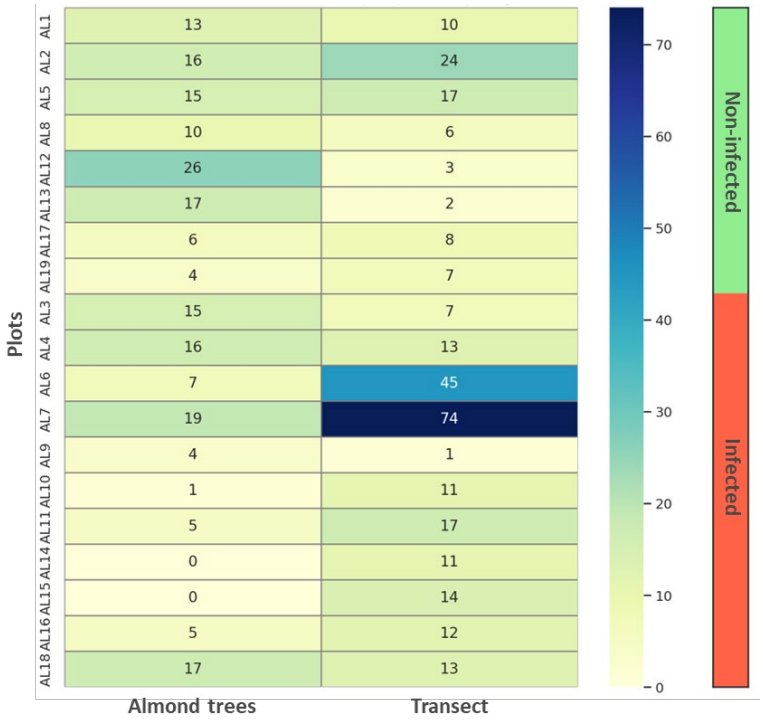


***Figure 4**: Heatmap showing the total number of Cicadellidae individuals per sampling plot, categorized by origin (almond tree vs. natural vegetation transect) and infection status (infected vs non-infected). Each cell represents the count of Cicadellidae in a given plot and microhabitat. Colour intensity corresponds to abundance, and infection status is indicated on the right.*

Cicadellidae counts were consistently lower in almond tree samples than in transects, regardless of infection status. This suggests that these vectors may preferentially occupy areas with denser or more structurally complex vegetation, such as the shrubland and forested zones represented by the transects, which likely provide more favourable microhabitats and resources.

To explore potential ecological drivers of vector presence and abundance, we analyzed the composition of plant species recorded in each natural vegetation transect. Plant species richness and the relative dominance of plant families were catalogued, and a multivariate correlation analysis was performed to investigate associations between plant community structure and hemipteran vector abundance. Preliminary results did not reveal consistent or significant correlations between vegetation composition and the abundance of Cicadellidae or Aphrophoridae. Moreover, no clear segregation of plots based on infection status emerged from the vegetation data. These findings suggest that, at the current resolution, vegetation structure alone does not explain vector distribution patterns.

Funded by the European Union

These observations underscore the need to further investigate the ecology and movement behavior of Cicadellidae in *Xf*-affected systems, particularly in relation to vegetation composition and disease presence. In addition to abundance and spatial distribution, we documented the morphological diversity of Hemiptera collected from both habitats. A selection of representative specimens was photographed to illustrate the variation in size, shape, and coloration observed across samples and morphotypes (**Figure 5**). These individuals were drawn from plots with varying infection statuses and both sampling habitats. These findings reinforce the need for COI barcoding to achieve genus- or species-level classification. Ongoing molecular analyses are expected to clarify species turnover between infected and non-infected plots and refine the understanding of vector distribution.

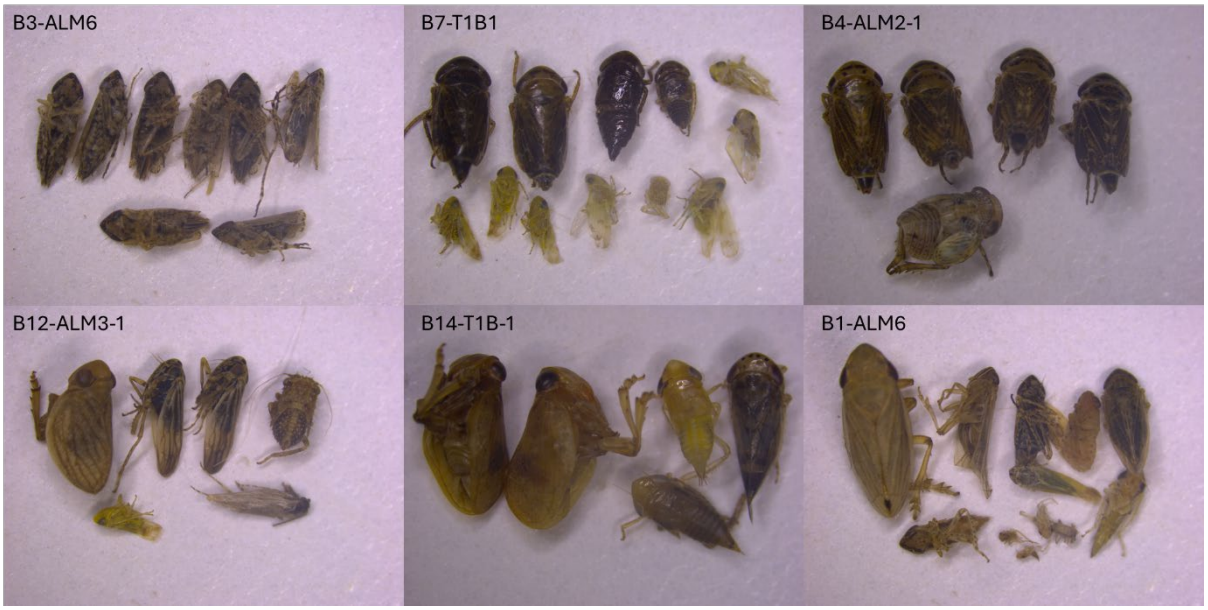


***Figure 5**: Representative specimens of Hemiptera collected from almond orchards and adjacent natural vegetation across different sampling plots. Each panel is labelled by plot and sample code: 'B' followed by a number indicates the plot, while 'T' or 'ALM' specify whether the sample was collected from a transect or beneath an almond tree. For transect samples, the following number (1 or 2) denotes the transect within the plot, and the letter (A or B) indicates the first or second 25-meter segment of that transect. For almond tree samples, the number represents the individual tree sampled (1 to 6). Selected morphotypes from these samples were chosen for COI molecular identification to achieve genus- or species-level resolution.*

Funded by the European Union

4. EFFECT OF *XYLELLA FASTIDIOSA* INFECTIONS AND ALMOND TREE ERADICATION ON SOIL QUALITY OF ALMOND ORCHARDS

Outbreaks of *Xf* in almond orchards have led to the implementation of strict eradication measures across several regions in the EU, including the compulsory removal of infected trees and, in some cases, the abandonment of agricultural land. While these measures are critical for containing the spread of this quarantine pathogen, their potential impact on soil quality remains poorly understood. The loss of tree cover, disruption of the root–soil interface, and incorporation of woody debris into the soil may alter both the physicochemical and biological properties of the soil, potentially affecting the long-term sustainability and resilience of these agroecosystems.

In addition, infected trees themselves may induce shifts in soil microbial communities prior to removal, due to altered root exudation patterns or stress-related changes in rhizosphere interactions. Understanding how both the presence of *Xf* infections and subsequent eradication measures influence soil quality is therefore essential for assessing the broader ecological impact of these current disease management practices.

In this section, we assessed the quality of soils collected from almond orchards with different *Xf* infection statuses and management histories. Specifically, we evaluated **physicochemical properties** (e.g., pH, organic matter content, nutrient availability), along with **biological soil properties**, including metabolic activity using isothermal microcalorimetry (SymCel CalScreener™ system) and functional diversity through Biolog EcoPlate™ profiling. In parallel, culturable bacterial populations were quantified using the dilution plating method. These complementary approaches aim to provide a comprehensive understanding of how *Xf* infections and eradication measures influence the physicochemical, functional, and microbial characteristics of soils in almond-producing regions.

4.1. Materials and methods

4.1.1. Soil sampling

Soil samples were collected from the same 19 almond field plots described in Section 2.1 from the canopy projection area of the six almond trees evaluated within each plot (**Figures 1, 6**). Additionally, soil samples were collected from seven almond plots where the presence of *Xf* had previously been confirmed and infected almond trees had been removed according to current phytosanitary regulations (**Figure 6**). In these eradicated plots, sampling was conducted at the exact locations occupied by at least six removed trees.

Following a standard protocol, the sampling point was marked, and the topsoil layer (approximately the upper 2–3 cm) was carefully cleared to remove organic debris (e.g., litter, plant residues) and inorganic material (e.g., stones, plastic fragments, or other waste). A hoe was then used to excavate to a depth of approximately 20 cm, from which a composite soil sample of about 1 kg was collected per sampling point. Samples were transported under

Funded by the European Union

appropriate conditions and subsequently processed and analyzed at the laboratories of the Institute for Sustainable Agriculture in Córdoba (IAS-CSIC).

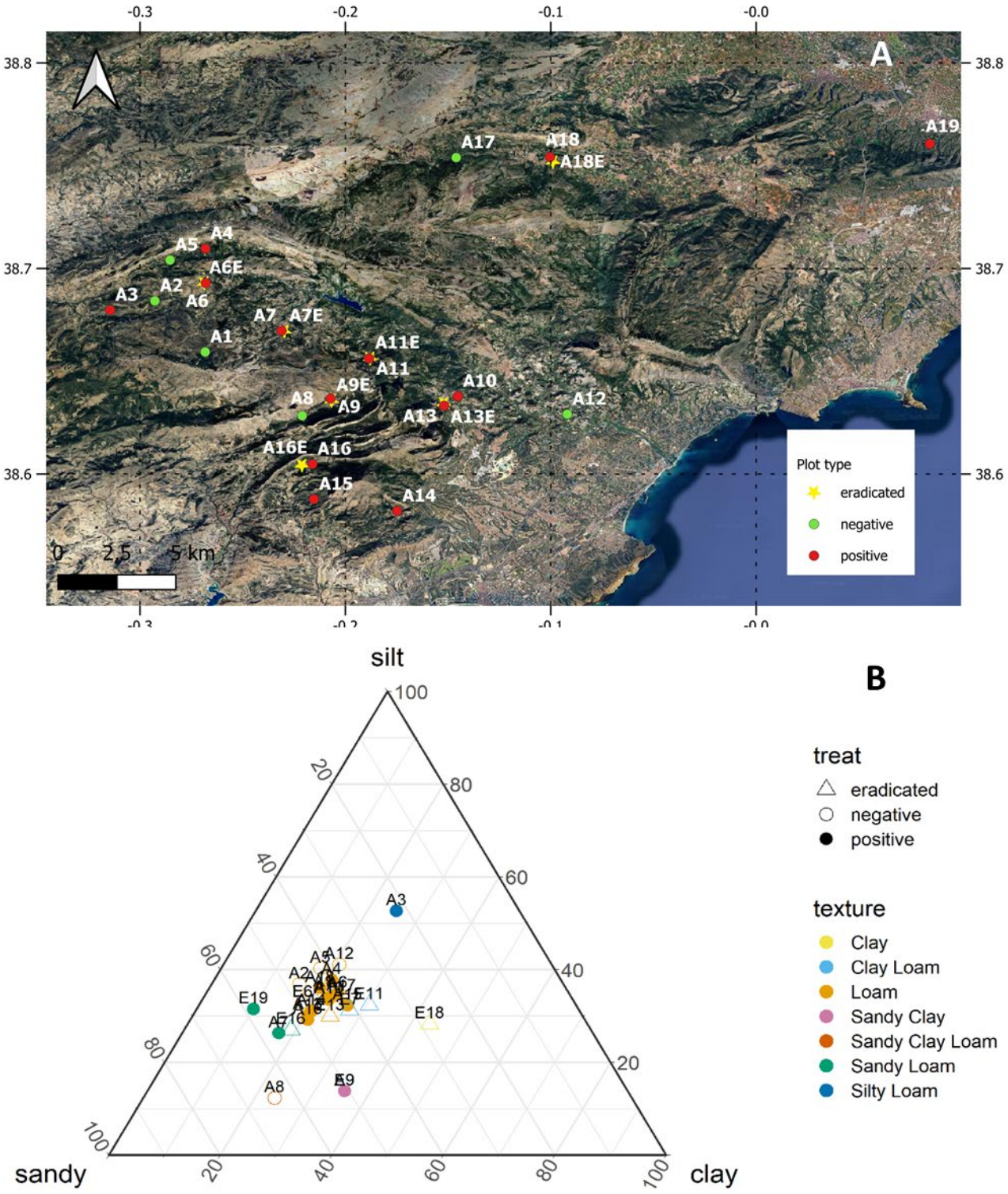


***Figure 6**: **A.** Geographic location of the 27 almond orchards sampled (including the eradicated ones) to assess the effect of* Xylella fastidiosa *infections and almond tree removal on soil quality. **B.** Soil textural class of the sampled almond orchards represented in the USDA soil texture triangle.*

Funded by the European Union

4.1.2. Soil physicochemical analysis

For each plot, the six individual soil samples were thoroughly mixed to obtain a composite sample. These composite samples were air-dried, passed through a 2 mm sieve and divided into subsamples for the physical, chemical and biological analyses indicated in **Table 7**. These subsamples were stored at 5 °C until analysis, for biological, physical and chemical properties. All physicochemical analyses were performed using standardized procedures (**Table 7**) by the Soil Analysis Service at IRNAS-CSIC (Seville, Spain; http://www.irnas.csic.es/).

Table 7. Methods used to determine the physical, chemical and biological soil parameters.

Parameters	Method
Physical parameters	
Clay (%)	
Sand (%)	Bouyoucos and Mick (1940)
Silt (%)	
Chemical parameters	
OM (%)	Walkley-Black (Stevenson, 1982)
Kjeldahl Nitrogen (% w/w)	Kjeldahl (Stevenson, 1982)
Extractable P (mg/kg)	Olsen (Olsen and Sommers, 1982)
Extractable K (mg/kg)	NH_4Cl (Reeve and Sumner, 1971)
Exchangeable Na (mg/kg)	Ammonium acetate method (volumetric)
Exchangeable Ca (mg/kg)	Ammonium acetate method (volumetric)
pH (H_2O)	1:2.5 suspension in water
E.C (mS/cm)	1:5 soil to water ratio (Rhoades, 1982)
$CaCO_3$ (%)	Gasometric method (Page et al.,1982)
C-Organic (%)	Walkley–Black method (Nelson and Sommers, 1982)
CEC (cmol/kg)	Ammonium replacement method (Rhoades, 1982)
Biological parameters	
Bacterial population	Culture-based dilution method (Montes-Borrego et al., 2013)
Soil metabolic activity	Isothermal microcalorimeter SymCel CalScreener™ system (Macan et al., unpublished results, 2025)
Soil functional diversity	Biolog EcoPlate™ system (Montes-Borrego et al., 2013)

4.1.3. Bacterial Population Densities

Soil suspensions were prepared by mixing 2.5 g of each soil sample with 25 mL of sterile saline solution in sterile Falcon tubes. Suspensions were shaken in an orbital shaker at 350 rpm for

Funded by the European Union

1 hour followed by centrifugation at 1000 g for 6 minutes, allowing the precipitation of soil particles. The resulting soil supernatant was then tenfold diluted in 0.85% saline solution and used for estimating bacterial population densitie sand the community-level physiological profile (CLPP) analysis with the Biolog EcoPlate™ system (Biolog Inc., Hayward, CA, USA) described in section 4.1.5.

Culturable bacterial populations were estimated using the dilution plating method. An aliquot of each dilution of the soil suspensions was serially diluted, and 100 µl of each dilution were plated in duplicate onto R2A agar. Plates were incubated at 28°C for 5-days, after which colony-forming-units (CFU) were quantified.

4.1.4. Isothermal microcalorimetry analysis

Overall soil metabolic activity was evaluated by an isothermal microcalorimeter (SymCel CalScreener™ system; SymCel Sverige AB, Stockholm, Sweden). This method relies on the continuous measurement of heat released during microbial metabolism. Briefly, 0.2-g of air-dried samples were weighed and transferred to sterile titanium vials in a laminar flow hood. Soil metabolic activity was measured after addition of autoclaved distilled water to reach 60% of the soil water holding capacity. Additionally, the experiment was repeated under the same conditions, except that the distilled water was replaced with the same amount of a glucose solution (30mg/mL). The vials were hermetically sealed and the calPlate was introduced into the equipment following manufacturer's protocol. Real-time heat production in each well was recorded at 30 ± 0.001°C for 48 h and expressed as heat flow over time (µW/h) using the calView™ software (Version 1.0.33.0, © 2015 SymCel, Sverige AB). At the end of the experiment, a metabolic profile (thermogram) was obtained for each well. Thermodynamic parameters derived from the power-time curves included: total heat (J/g soil), metabolic rate (µW), time to peak (h), peak heat flow (µW/g soil), accumulated heat at 10 hours (J/g soil), and the time (h) required to reach each increment of 1 J/g soil.

4.1.5. Bacterial Community level physiological profiles

For analysing the CLPP of each soil an aliquot of 150 µl of the soil supernatant was added to each well, with a total of three biological replicates per almond orchard that were assessed using the same 96-well EcoPlates, which consist of 31 different carbon sources in triplicates. Inoculated plates were incubated at 28°C, and the absorbance was measured at 590 nm with a Tecan Safire fluorospectrometer (Tecan Spain, Barcelona, Spain) at 12 hour intervals for 7 days. Average well color development (AWCD) was calculated as the mean absorbance values of all 31 response wells per reading time. The metabolic diversity of the bacterial community was assessed by comparing the CLPPs of all replicates and treatments at 72 h, corresponding to the average inflection point of the AWCD curve, and at the end of the incubation period (Montes-Borrego et al.,2013).

Funded by the European Union

4.1.6. Statistical analysis

All assessed parameters were first tested for normality using the Shapiro-Wilk test and for homogeneity of variances using Levene's test. Parameters meeting the assumptions of normally and homoscedasticity were analysed using One-Way ANOVA followed by Tukey's HSD post-hoc test for pairwise comparisons at $P < 0.05$. For parameters not meting these assumptions, the Kruskal-Wallis test was applied, and significant results were further examined with Dunn's test at $P < 0.05$. All analyses and graphical outputs were performed in R version 4.2.0 using the ggplot2, ggpubr, tidyr, and rstatix packages.

4.2 Results

4.2.1 Soil physicochemical analysis

The soils of the 26 almond orchards displayed a heterogeneous textural composition, ranging from loamy to clay-rich types (Figure 6B). The majority of orchards (over half of the samples) were classified as **loam**, reflecting balanced proportions of sand, silt, and clay, typically with clay contents between 20–25%. Several orchards presented finer textures, such as **clay loam** (e.g., the eradicated orchards E11, E7) and **clay** (E18), with clay fractions exceeding 30–40%. In contrast, coarser textures were also identified, including **sandy loam** (e.g., E16, A19, A7) and **sandy-clay** (A9 and E9), with higher sand contents (>30–40%). A smaller number of orchards exhibited **silty-loam** (A3) and **loam–clay–sand** mixture (A8). This variability in soil texture, from sandy loams to clay-dominated soils, highlights the strong edaphic heterogeneity across the study area, which may influence water retention, nutrient availability, and microbial community dynamics in almond orchards. Overall, this variability in soil texture across the orchards may provide different context for interpreting differences in soil physicochemical properties, microbial activity, and the potential influence on *Xylella fastidiosa* dynamics.

Soil physicochemical parameters varied among almond orchards with different *Xf* statuses (**Figure 7**). Available calcium, available potassium, and cation exchange capacity (CEC) were significantly higher ($P<0.05$) in soils from eradicated plots than in non-eradicated *Xf*-positive plots, with non-eradicated *Xf*-negative plots showed intermediate values. In contrast, total carbon were highest ($P<0.05$) in soils from non-eradicated *Xf*-negative plots and lowest in eradicated plots, while non-eradicated *Xf*-positive plots had intermediate values. $CaCO_3$ content was also greater ($P<0.05$) in non-eradicated *Xf*-positive soils compared with both eradicated and non-eradicated *Xf*-negative soils. Phosphorus content was highest ($P<0.05$) in non-eradicated *Xf*-negative soils, with lower levels ($P\geq0.05$) in non-eradicated *Xf*-positive and eradicated plots. No significant differences among treatments were detected for available magnesium, organic matter, C-organic, total nitrogen, CE, or pH (**Figure 7**).

Funded by the European Union

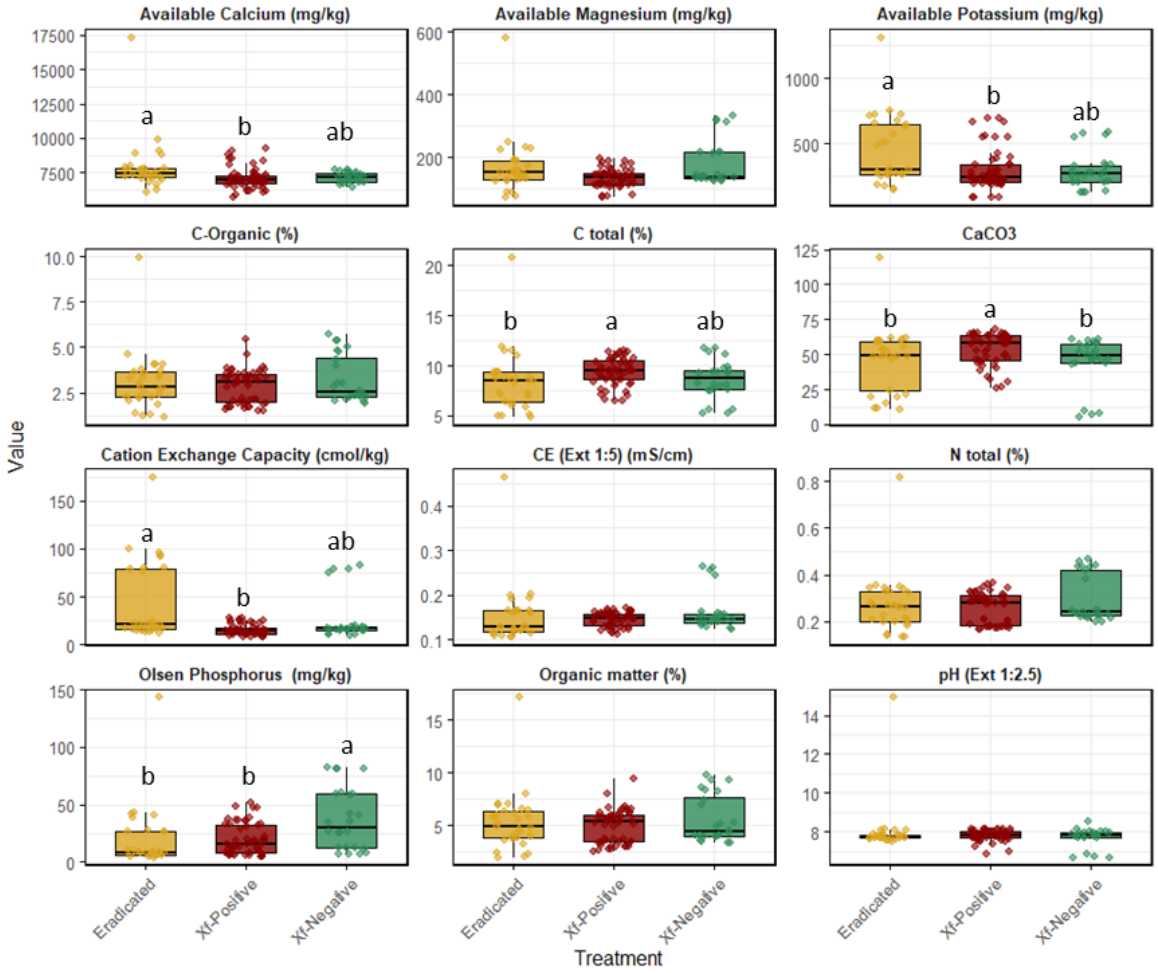


Figure 7. *Boxplots of soil physicochemical parameters in almond orchards grouped according to* Xylella fastidiosa *(*Xf*) infection status: non-eradicated* Xf*-negative, non-eradicated* Xf*-positive, and eradicated plots. Different letters above the boxes indicate significant differences among groups according to Kruskal-Wallis followed by Dunn test at P<0.05. Parameters without letters showed no significant differences.*

PCA of all measured physicochemical parameters (**Figure 8**) showed no consistent overall separation among *Xf* infection or eradication statuses. Nonetheless, some plots showed distinct profiles at the individual plot level between eradicated and non-eradicated sites. These site-level differences may be linked to specific textural or physicochemical properties of the soil that could result in the changes in the soil microbial community composition and activity described in the subsequent sections.

Funded by the European Union

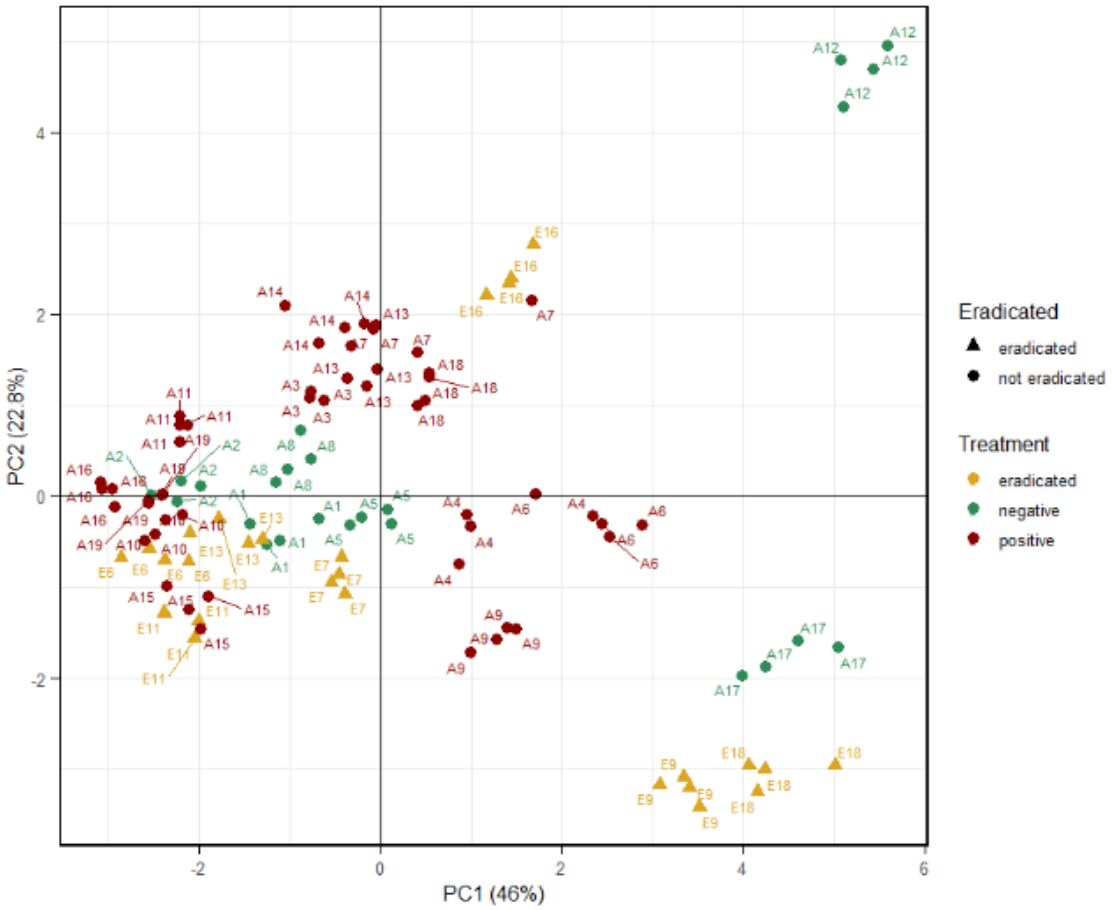


Figure 8. *Principal Components Analysis (PCA) of physicochemical parameters in the 27 almond orchards grouped according to their* Xylella fastidiosa *and eradication status. Percent variance explained by each axis is indicated in parentheses.*

4.2.2 Bacterial Population Densities

The density of culturable bacteria in soils from almond orchards, estimated by the dilution technique, ranged from 4.76±0.20 to 6.21±0.08 log CFU g^{-1} of soil across the assessed orchards (Figure 9A).

When grouped by *Xf* infection and eradication status, soil samples from *Xf*-negative plots had a significantly higher number of culturable bacteria than those from *Xf*-positive orchards (*P*=0.034). However, no significant differences were found between *Xf*-negative and eradicated samples or between eradicated and *Xf*-positive samples (*P* > 0.61) (Figure 9B).

Funded by the European Union

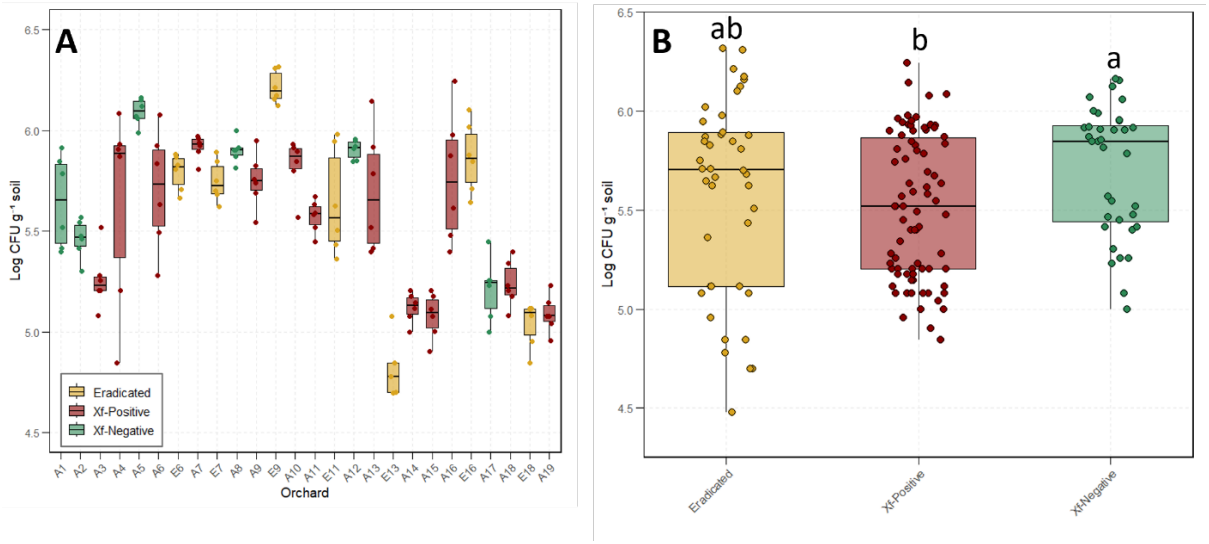


Figure 9. *Boxplots of population density of culturable bacteria (log CFU g^{-1} soil) in almond orchard soils. (**A**) Distribution across the 19 individual orchards, and (**B**) grouped by* Xylella fastidiosa *infection status and tree eradication at the time of sampling. Different letters indicate significant differences among groups (*P *< 0.05, Kruskal-Wallis followed by Dunn test).*

4.2.3 Isothermal microcalorimetry analysis

The overall metabolic activity of the soil samples was assessed using isothermal microcalorimetry. Figure 10 presents the thermograms recorded for each sample under basal conditions (without glucose amendment) and their stimulated activity after glucose addition. Across all orchards, glucose addition produced a markedly higher heat flow peaks than basal activity, indicating enhanced microbial respiration when a carbon source like glucose was supplied.

At individual orchard level, when comparing nearby orchards where soil samples were collected from both eradicated and non-eradicated plots , orchards 6, 7, 11, and 13 tended to show lower metabolic activity in eradicated zones than non-eradicated ones. In contrast, no clear differences in thermogram profiles between eradicated and non-eradicated status were observed in orchards 9, 16, and 18 (Figure 10).

Accumulated heat curves calculated from glucose-amended soil samples are presented in Figure 11. Parameters derived from both the heat flow and accumulated heat curves are included time to peak (h), peak heat flow (µW/g soil), total heat (J/g soil), metabolic rate (µW), accumulated heat at 10 hours (J/g soil), and the time (h) required to reach each increment of 1 J/g soil and are summarized in Table 8.

Funded by the European Union

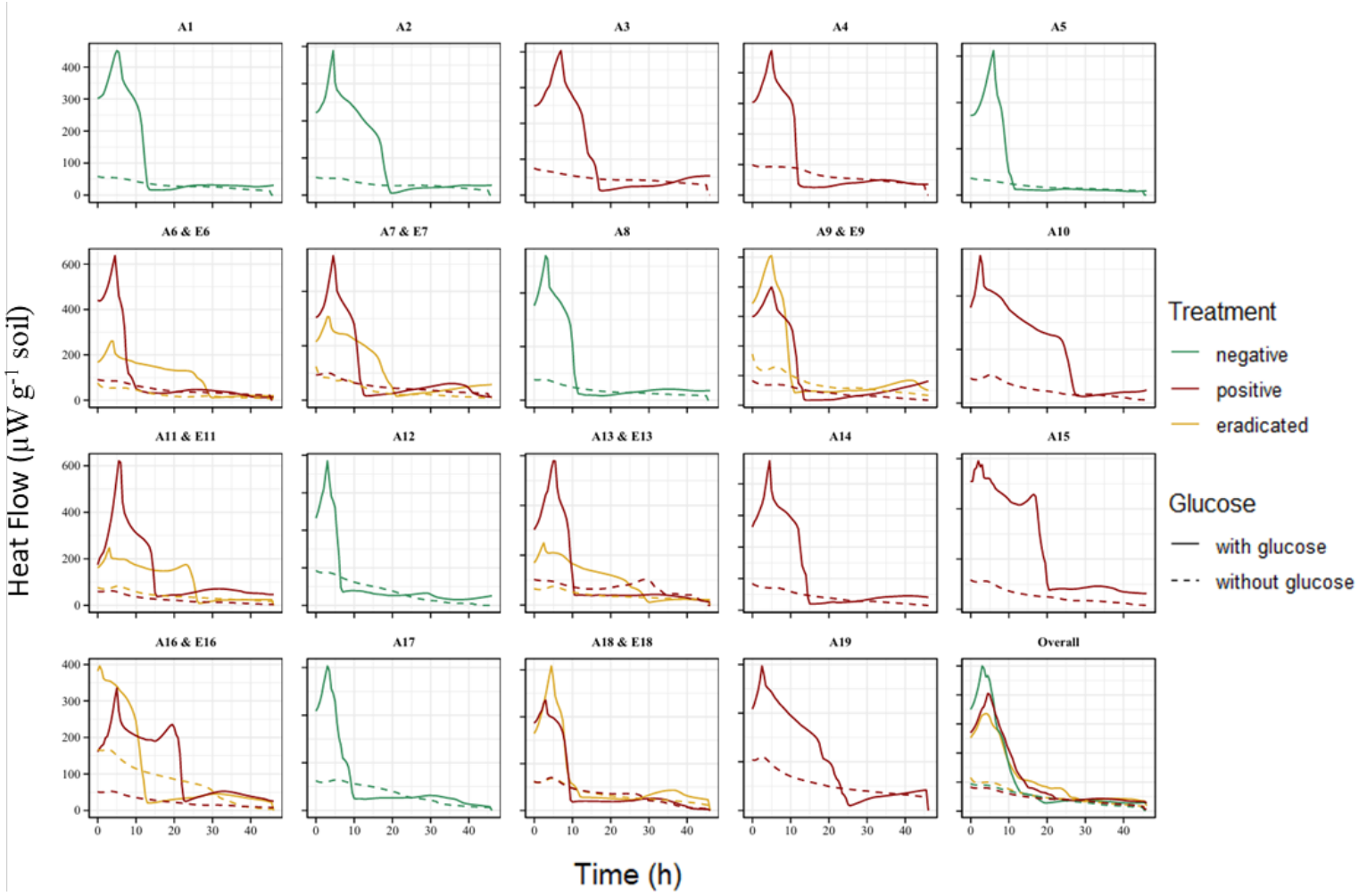


Figure 10. *Heat flow curves for each soil sample monitored by isothermal microcalorimetry, colored according to Xf infection and almond tree eradication status. Dashed lines show basal microbial activity, and solid lines show glucose-stimulated microbial activity.*

Funded by the European Union

Table 8. Parameters derived from the heat flow and accumulated heat curves using isothermal microcalorimetry for each orchard status

Status of almond orchard	Total heat (J/g soil)	Metabolic rate (µW)	Time to peak (h)	Peak heat flow (µW/g soil)	Accumulated heat at 10h (J/g soil)	Time to reach 1 J/g soil (h)
***Xf*-Negative**	18.41 ± 1.63	111.19 ± 9.85	4.23 ± 1.2 ab	566.12 ± 130.31 a	13003.8 ± 1650.08 a	1.10 ± 0.21 b
***Xf*-Positive**	18.95 ± 2.26	114.42 ± 13.63	4.38 ± 1.44 a	449.15 ± 123.7 b	11454.51 ± 2361.07 b	1.27 ± 0.32 ab
Eradicated	18.45 ± 2.46	111.44 ± 14.87	3.23 ± 1.36 b	371.5 ± 141.32 c	10060.53 ± 3069.49 b	1.45 ± 0.42 a

Funded by the European Union

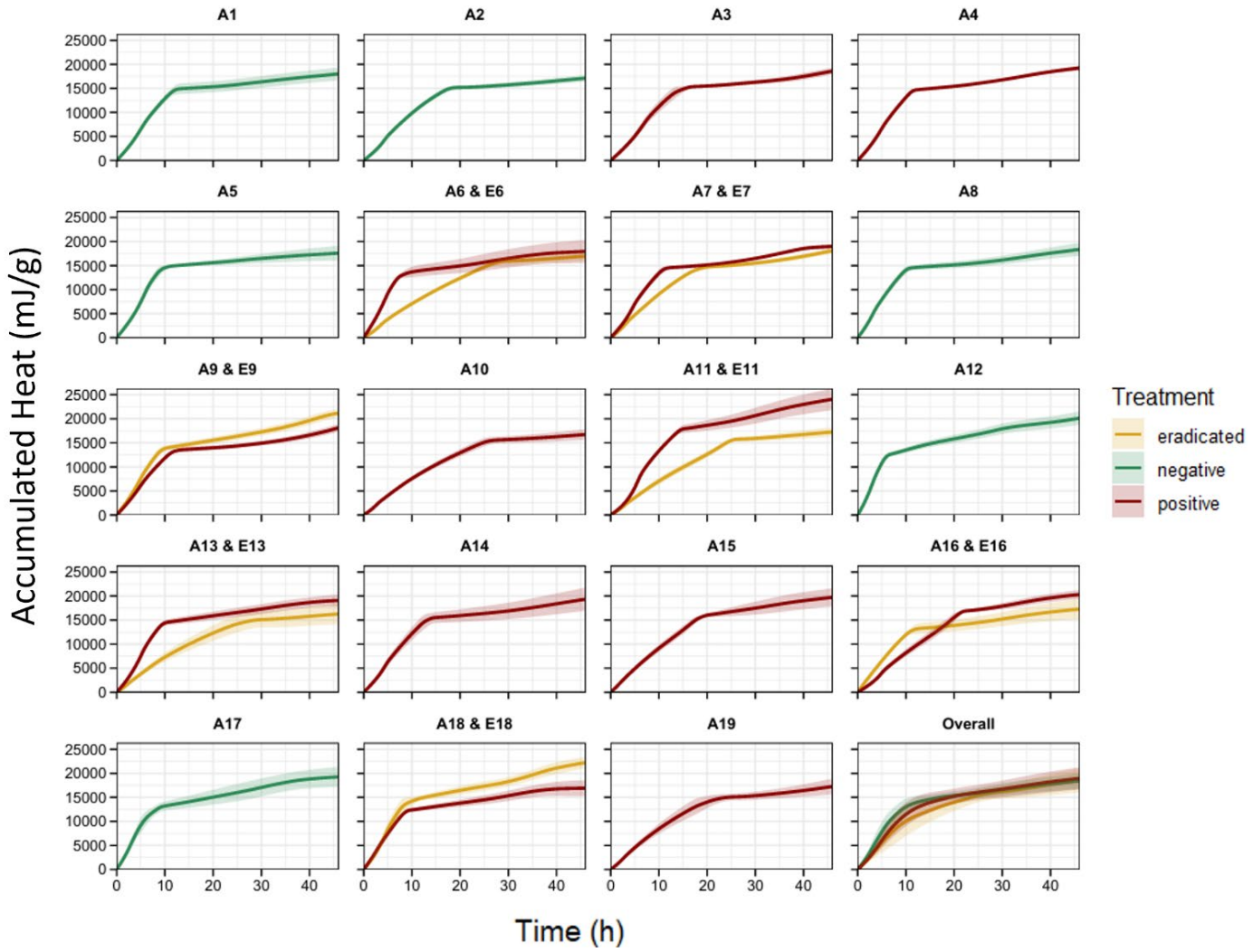


Figure 11. *Accumulated heat (mJ g^{-1} soil) curves measured by isothermal microcalorimetry (CalScreener). Lines show the mean of four replicates, with shaded areas indicating the standard deviation.*

Funded by the European Union

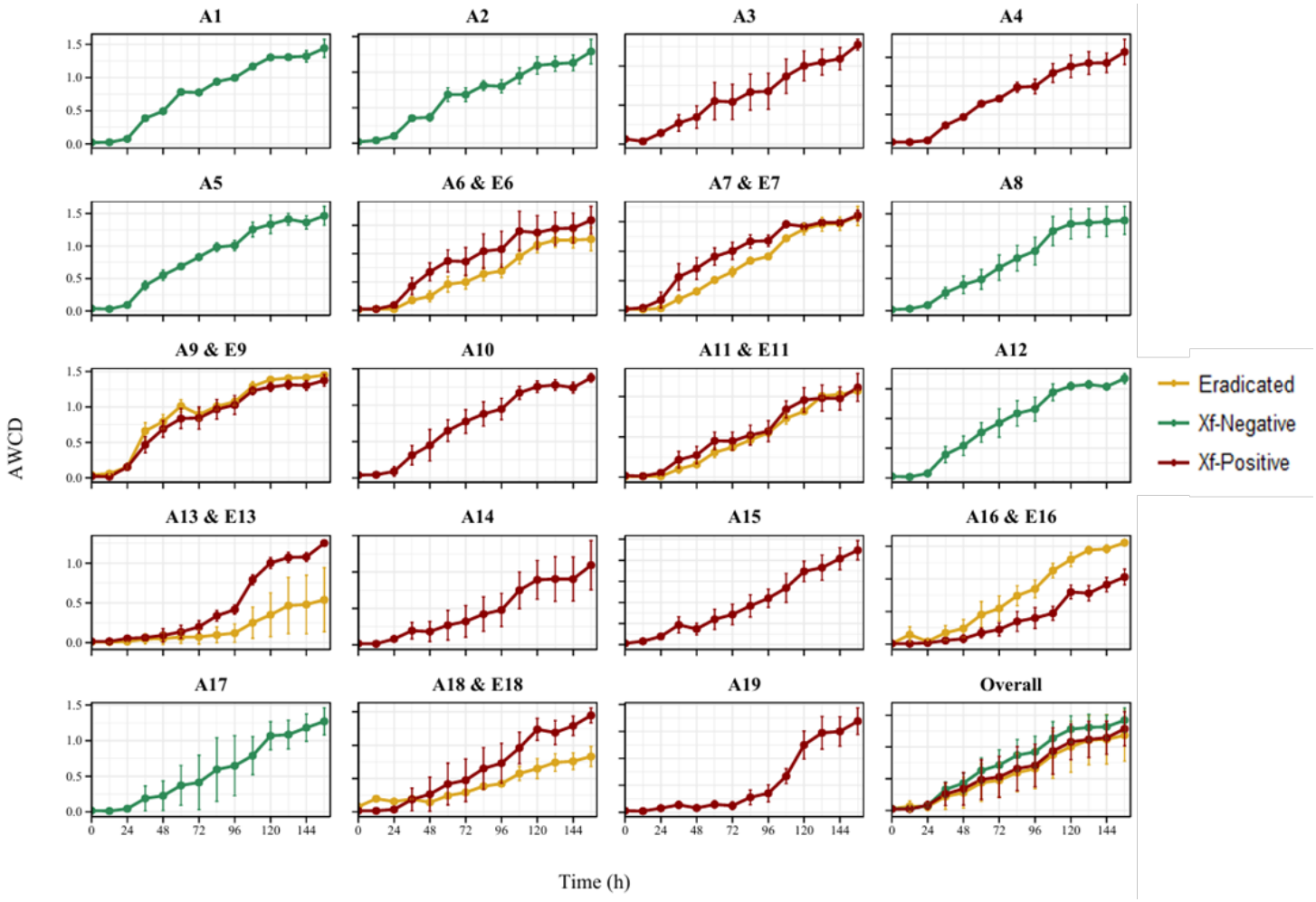


Figure 12. *Average Well Color Development (AWCD) curves, measured as optical density at 590 nm (OD590), representing substrate utilization profiles in Biolog EcoPlates for each assessed orchard. Error bars show standard deviations of replicate wells.*

Funded by the European Union

Total heat production and metabolic rate did not differ significantly among *Xf*-status and eradicated zones ($P = 0.508$). In contrast, the time to reach peak heat flow was significantly longer in soils from *Xf*-positive zones than from eradicated ones ($P = 0.006$). Moreover, peak heat flow was highest in *Xf*-negative soils, intermediate in *Xf*-positive and lowest in eradicated zones ($P < 0.033$) (Table 8). Accumulated heat at 10 h followed a similar trend, with greater values in Xf-negative soils, while the time to reach 1 J/g soil was longest in eradicated soils. Thus, despite overall metabolic activity was similar across treatments, these differences in peak heat flow and time to peak indicate altered microbial responses to glucose amendment, potentially reflecting shifts in microbial community structure and composition. Such patterns could be further investigated using molecular sequencing approaches.

4.2.4 Bacterial Community level physiological profiles

Soil metabolic activity was further assessed using community-level physiological profiles (CLPP) from Biolog EcoPlates, which evaluates the functional diversity of soil microbial communities. The Average Well Color Development (AWCD) curves derived from absorbance measurements of 31 carbon substrates, is shown in Figure 12, providing an indicator of overall soil metabolic activity.

Consistent with the isothermal microcalorimetry results (Figure 11), soil samples from orchards 6, 7, and 13 exhibited lower activity in eradicated areas compared to non-eradicated plots, while orchard 18 showed a similar trend. In contrast, orchards 9 and 11 displayed similar activity between eradicated and non-eradicated samples, being orchard 16 the only site with opposite trend, with higher activity in soils from eradicated areas (Figure 12).

Metabolic diversity indices presented in Figure 13 indicated higher metabolic richness ($P < 0.02$) and diversity ($P < 0.01$) in *Xf*-negative samples than both *Xf*-positive and eradicated soils, indicating a broader range and variety of metabolized substrates. Evenness values did not differ significantly among treatments.

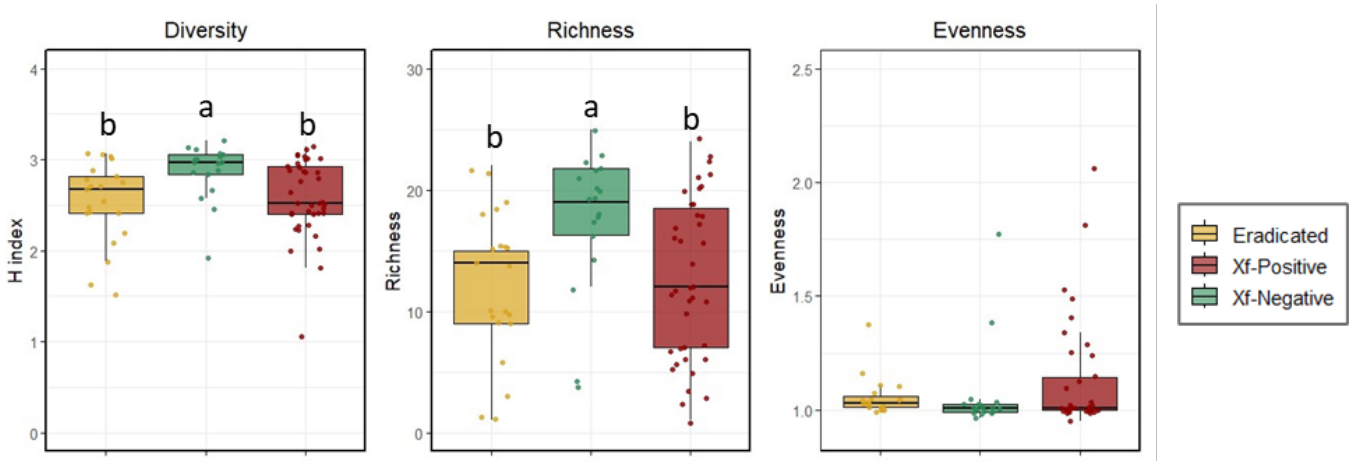


Figure 13. *Functional metabolic alpha diversity indices calculated after 72 h of Ecoplate incubation. Different letters indicate significant differences among treatments (*P *< 0.05, Tukey's HSD test).*

Funded by the European Union

Principal Component Analysis (PCA) of the 31 carbon utilization profiles (Figure 14) did not revealed clear clustering associated with either eradication status or *Xf*-infection status, suggesting that these factors did not substantially influence the overall metabolic profile of the soil microbial communities in soil samples.

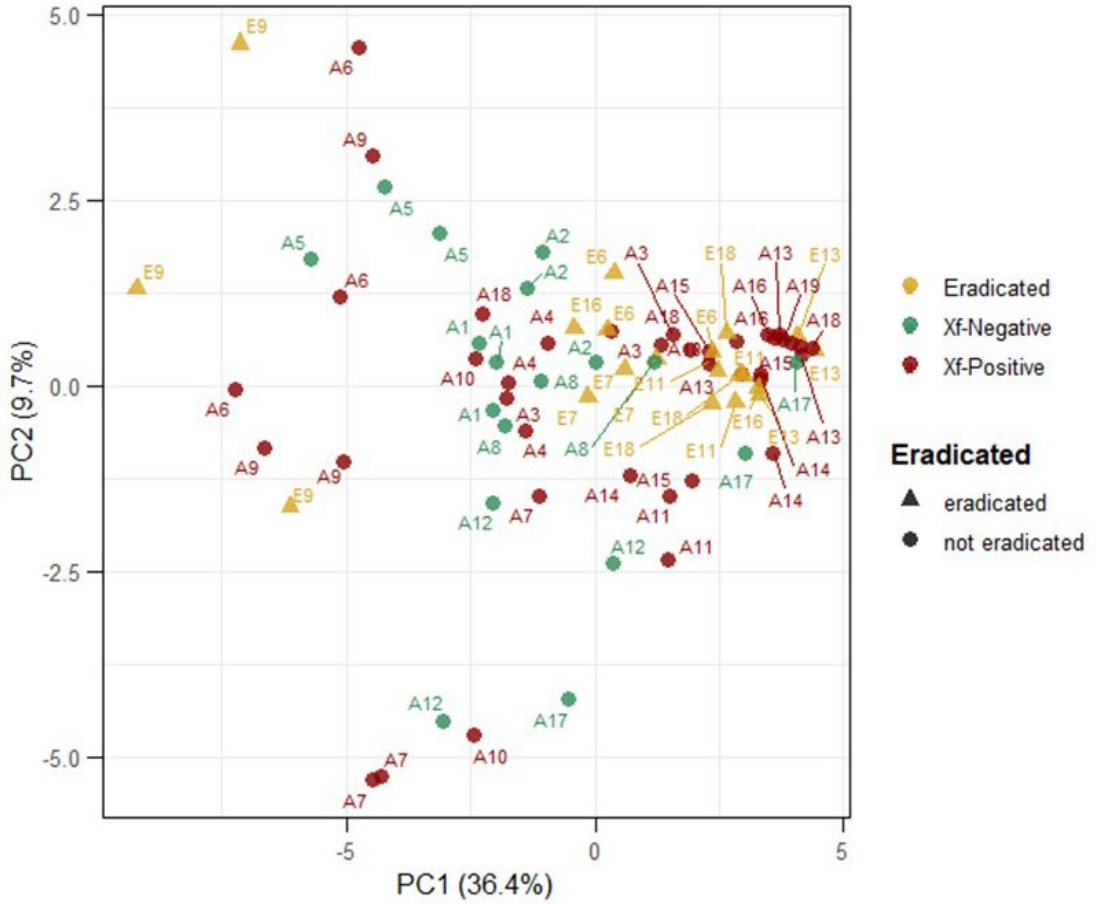


Figure 14. *Principal Components Analysis (PCA) of 31 carbon source utilization profiles after 72 h of Ecoplate incubation. Each point represents a soil sample; distances reflect similarity in carbon utilization patterns.*

Funded by the European Union

5. GENERAL CONCLUSIONS

Our findings reveal that *Xylella fastidiosa* dynamics in almond agroecosystems are shaped by a complex interplay between environmental conditions, vegetation structure, vector communities, and soil properties.

In almond orchards, the combined effects of *Xf* infection and environmental factors—such as drought, shrub cover, and landscape fragmentation—had a marked impact on tree health. In contrast, in the surrounding natural vegetation, abiotic stressors, particularly temperature and water availability, had a stronger influence on plant health than *Xf* infection itself. Interestingly, the forest-agriculture interface played a significant role in almond health. The abundance of *Xf* host plants in the surrounding natural vegetation was positively associated with almond defoliation, which was exacerbated in *Xf* infected plots. However, plant diversity was not significantly associated with tree health, indicating that *Xf*-related damage is influenced by multiple interacting drivers.

Vector monitoring indicated that Cicadellidae, the most abundant potential vector group, were more common in structurally complex natural vegetation than within orchards, with slightly higher numbers in infected areas. Although no strong statistical link between vector abundance and *Xf* presence at family level, these patterns, together with the occurrence of Aphrophoridae, underscore the need for continued, species-specific surveillance to better understand transmission pathways.

Soil analyses indicated that both *Xf* infection and eradication measures can influence soil biological properties. *Xf*-negative orchards typically showed higher culturable bacterial populations, greater metabolic diversity, and higher peak microbial activity following glucose amendment. Eradicated plots often exhibited reduced functional diversity and slower microbial responses, suggesting potential long-term effects on soil health. These shifts may affect ecosystem resilience and recovery after eradication, emphasizing the need of integrating soil conservation measures into phytosanitary strategies.

Overall, the results highlight that effective *Xf* management should extend beyond tree-level interventions. A landscape-scale, multi-trophic approach addressing vector ecology, surrounding vegetation management, soil health, and climatic stressors in an integrated manner is needed. Such an approach will improve the resilience of almond production systems and help safeguard both agricultural productivity and biodiversity at the forest–agriculture interface.

Funded by the European Union

6. REFERENCES

Alexander H.M., Mauck, K.E., Whitfield A.E., Garrett, K.A., Malmstrom C.M., 2014. Plant-virus interactions and the agro-ecological interface. European Journal of Plant Pathology 138, 529–547. https://doi.org/10.1007/s10658-013-0317-1

Alfaro García P., Andreu Rodes J.M., Bautista S., Delgado J., Soria Mingorance J.M., 2004. Riesgos geológicos en la provincia de Alicante. Universidad de Alicante. Instituto de Ciencias de la Educación.

Barton, K., 2022. MuMIn: Multi-model inference. R package version 1.47.1. http://CRAN.R-project.org/package=MuMIn

Bonants P., Griekspoor Y., Houwers, I., Krijger M., van der Zouwen P., van der Lee T.A.J., van der Wolf J., 2019. Development and Evaluation of a Triplex TaqMan Assay and Next-Generation Sequence Analysis for Improved Detection of Xylella in Plant Material. Plant Disease 103, 645–655. https://doi.org/10.1094/PDIS-08-18-1433-RE

Bouyoucos G. J., & Mick A. H., 1940. *An electrical resistance method for the continuous measurement of soil moisture under field conditions* (Technical Bulletin No. 172). Michigan State College Agricultural Experiment Station.

Burdon J.J., Zhan, J., 2020. Climate change and disease in plant communities. PLOS Biology 18, e3000949. https://doi.org/10.1371/journal.pbio.3000949

Burnham K.P., Anderson D.R., 2002. Model selection and multimodel inference: a practical information-theoretic approach. Springer, New York, USA.

Cornara D., Morente M., Markheiser A., Bodino, N., Tsai C.-W., Fereres A., Redak R.A., Perring T.M., Lopes J.R.S., 2019. An overview on the worldwide vectors of *Xylella fastidiosa*. Entomologia Generalis 39, 157–181. https://doi.org/10.1127/entomologia/2019/0811

De la Fuente L., Navas-Cortés J.A., Landa B.B., 2024. Ten Challenges to Understanding and Managing the Insect-Transmitted, Xylem-Limited Bacterial Pathogen *Xylella fastidiosa*. Phytopathology 114, 869-884. https://doi.org/10.1094/PHYTO-12-23-0476-KC

Decocq G., Andrieu E., Brunet J., Chabrerie O., De Frenne P., De Smedt P., Deconchat M., Diekmann M., Ehrmann S., Giffard B., Mifsud E.G., Hansen K., Hermy M., Kolb A., Lenoir J., Liira J., Moldan F., Prokofieva I., Rosenqvist L., Varela, E., Valdés A., Verheyen K., Wulf M., 2016. Ecosystem Services from Small Forest Patches in Agricultural Landscapes. Current Forestry Reports 2, 30–44. https://doi.org/10.1007/s40725-016-0028-x

Duguy B., Vallejo V.R., 2008. Land-use and fire history effects on post-fire vegetation dynamics in eastern Spain. Journal of Vegetation Science 19, 97–108.

EFSA, E.F.S., Cavalieri V., Fasanelli E., Furnari G., Gibin D., Gutierrez Linares A., La Notte P., Pasinato L., Stancanelli G., Delbianco A., 2025. Update of the *Xylella* spp. host plant database – Systematic literature search up to 30 June 2024. EFSA Journal 23, e9241. https://doi.org/10.2903/j.efsa.2025.9241

Eichhorn J., Roskams, P., Potocic N., Timmermann V., Ferretti M., Mues, V., Szepesi A., Durrant D., Seletkovic I., Schroeck H.-W., 2016. Part IV Visual assessment of crown condition and

Funded by the European Union

damaging agents. Manual on methods and criteria for harmonized sampling, assessment, monitoring and analysis of the effects of air pollution on forests.

EPPO, 2023. PM 7/24 (5) *Xylella fastidiosa.* EPPO Bulletin 53, 205–276. https://doi.org/10.1111/epp.12923

Evans J.S., Oakleaf J., Cushman S.A., Theobald D., 2014. An ArcGIS toolbox for surface gradient and geomorphometric modeling, version 2.0-0. Available: http://evansmurphy.wix.com/evansspatial . Accessed: 2017 Dec.

Gilbert G.S., 2002. Evolutionary ecology of plant diseases in natural ecosystems. Annual Review of Phytopathology 40, 13–43. https://doi.org/10.1146/annurev.phyto.40.021202.110417

Gilbert G.S., Parker I., 2023. The Evolutionary Ecology of Plant Disease. O*x*ford University Press.

Greco D., Aprile A., De Bellis L., Luvisi A., 2021. Diseases Caused by *Xylella fastidiosa* in *Prunus Genus:* An Overview of the Research on an Increasingly Widespread Pathogen. Frontiers in Plant Science 12, 712452. https://doi.org/10.3389/fpls.2021.712452

GVA, 2024. Situación de *Xylella fastidiosa* en la Comunitat Valenciana. Servicio de Sanidad Vegetal, DG Agricultura, Ganadería y Pesca, Generalitat Valenciana. [WWW Document]. Portal Agrari. URL https://portalagrari.gva.es/va/agricultura/xylella-fastidiosa (accessed 3.25.25).

Harper S.J., Ward L.I., Clover G.R.G., 2010. Development of LAMP and real-time PCR methods for the rapid detection of *Xylella fastidiosa* for quarantine and field applications. Phytopathology 100, 1282–1288. https://doi.org/10.1094/PHYTO-06-10-0168

Hernández-Lambraño R.E., González-Moreno P., Sánchez-Agudo J.Á., 2018. Environmental factors associated with the spatial distribution of invasive plant pathogens in the Iberian Peninsula: The case of *Phytophthora cinnamomi* Rands. Forest Ecology and Management 419–420, 101–109. https://doi.org/10.1016/j.foreco.2018.03.026

Hesselbarth M.H.K., Sciaini M., With K.A., Wiegand K., Nowosad J., 2019. Landscapemetrics: an open-source R tool to calculate landscape metrics. Ecography 42, 1648–1657. https://doi.org/10.1111/ecog.04617

Johnson P.T.J., Ostfeld R.S., Keesing F., 2015. Frontiers in research on biodiversity and disease. Ecology Letters 18, 1119–1133. https://doi.org/10.1111/ele.12479

Kelley C., Ting, M., Seager R., Kushnir Y., 2012. Mediterranean precipitation climatology, seasonal cycle, and trend as simulated by CMIP5. Geophysical Research Letters 39, L21703. https://doi.org/10.1029/2012GL053416

Montes-Borrego M., Navas-Cortés J. A., Landa, B. B., (2013). Linking microbial functional diversity of olive rhizosphere soil to management systems in commercial orchards in southern Spain. Agriculture, Ecosystems & Environment 181, 169–178. https://doi.org/10.1016/j.agee.2013.09.021

Mordecai E.A., 2011. Pathogen impacts on plant communities: unifying theory, concepts, and empirical work. Ecological Monographs 81, 429–441. https://doi.org/10.1890/10-2241.1

Funded by the European Union

Nelson D. W., & Sommers L. E., 1982. Total carbon, organic carbon, and organic matter. In A. L. Page, R. H. Miller, & D. R. Keeney (Eds.), *Methods of soil analysis: Part 2 chemical and microbiological properties* (pp. 539–579). American Society of Agronomy.

Oksane J., Simpson G.L., Blanchet F.G., Kindt R., Legendre P., Minchin P.R., O'Hara R.B., Solymos P., Stevens M.H.H., Szoec, E., Wagner H., Barbour M., Bedward M., Bolker B., Borcard D., Carvalho G., Chirico M., Caceres M.D., Durand S., Evangelista H.B.A., FitzJohn R., Friendly M., Furneaux,B., Hannigan,G., Hill M.O., Lahti L., McGlinn D., Ouellette M.-H., Cunha E.R., Smith T., Stier A., Braak C.J.F.T., Weedon J., 2022. vegan: Community Ecology Package.

Olsen S. R., Sommers L. E., 1982. Phosphorus. In A. L. Page, R. H. Miller, & D. R. Keeney (Eds.), *Methods of soil analysis: Part 2 chemical and microbiological properties* (pp. 403–430). American Society of Agronomy. https://doi.org/10.2134/agronmonogr9.2.2ed.c24

Ouyang P., Arif M., Fletcher J., Melcher U., Ochoa Corona F.M., 2013. Enhanced reliability and accuracy for field deployable bioforensic detection and discrimination of *Xylella fastidiosa* subsp. *pauca*, causal agent of citrus variegated chlorosis using razor ex technology and TaqMan quantitative PCR. PloS One 8, e81647. https://doi.org/10.1371/journal.pone.0081647

Page A. L., Miller R. H., Keeney D. R., 1982. *Methods of soil analysis Part 2—Chemical and microbiological properties* (2nd ed.). American Society of Agronomy.

Pandey P., Irulappan V., Bagavathiannan M.V., Senthil-Kumar M., 2017. Impact of Combined Abiotic and Biotic Stresses on Plant Growth and Avenues for Crop Improvement by Exploiting Physio-morphological Traits. Frontiers in Plant Science 8, 537. https://doi.org/10.3389/fpls.2017.00537

Pinheiro J., Bates, D., DebRoy S., Sarkar D., Team R.C., 2020. nlme: Linear and nonlinear mixed effects models. R package version 3.1-150, https://CRAN.R-project.org/package=nlme .

R Core Team, 2019. R: A language and environment for statistical computing. R Foundation for Statistical Computing, Vienna, Austria. URL https://www.R-project.org/.

Reeve N. G., & Sumner M. E., 1971. Cation exchange capacity and exchangeable aluminum in Natal oxisols. Soil Science Society of America Journal 35, 38–42. https://doi.org/10.2136/sssaj1971.03615995003500010017x

Rhoades J. D., 1982. Soluble salts. In A. L. Page, R. H. Miller, & D. R. Keeney (Eds.), *Methods of soil analysis: Part 2 chemical and microbiological properties* (pp. 167–179). American Society of Agronomy.

Ristaino J.B., Anderson P.K., Bebber D.P., Brauman K.A., Cunniffe N.J., Fedoroff N.V., Finegold C., Garrett K.A., Gilligan C.A., Jones C.M., Martin M.D., MacDonald G.K., Neenan P., Records A., Schmale D.G., Tateosian L., Wei Q., 2021. The persistent threat of emerging plant disease pandemics to global food security. Proceedings of the National Academy of Sciences 118, e2022239118. https://doi.org/10.1073/pnas.2022239118

Roossinck M.J., García-Arenal F., 2015. Ecosystem simplification, biodiversity loss and plant virus emergence. Current opinion in virology 10, 56–62. https://doi.org/10.1016/j.coviro.2015.01.005

Funded by the European Union

Schneider K., Mourits M., van der Werf W., Lansink A.O., 2021. On consumer impact from *Xylella fastidiosa* subspecies *pauca*. Ecological Economics 185, 107024. https://doi.org/10.1016/j.ecolecon.2021.107024

Sicard A., Saponari M., Vanhove M., Castillo A.I., Giampetruzzi A., Loconsole G., Saldarelli P., Boscia D., Neema C., Almeida R.P.P., 2021. Introduction and adaptation of an emerging pathogen to olive trees in Italy. Microbial genomics 7, 000735. https://doi.org/10.1099/mgen.0.000735

Sicard A., Zeilinger A.R., Vanhove M., Schartel T.E., Beal D.J., Daugherty M.P., Almeida R.P.P., 2018. *Xylella fastidiosa:* Insights into an Emerging Plant Pathogen. Annual Review of Phytopathology 56, 181–202. https://doi.org/10.1146/annurev-phyto-080417-045849

Singh B.K., Delgado-Baquerizo M., Egidi, E., Guirado E., Leach J.E., Liu H., Trivedi P., 2023. Climate change impacts on plant pathogens, food security and paths forward. Nature Reviews Microbiology 21, 640–656. https://doi.org/10.1038/s41579-023-00900-7

Stevenson F. J., 1982. Nitrogen-organic forms. In A. L. Page, R. H. Miller, & D. R. Keeney (Eds.), *Methods of soil analysis: Part 2 chemical and microbiological properties* (pp. 625–641). American Society of Agronomy.

Teshome D.T., Zharare G.E., Naidoo S., 2020. The Threat of the Combined Effect of Biotic and Abiotic Stress Factors in Forestry Under a Changing Climate. Frontiers in Plant Science 11, 601009. https://doi.org/10.3389/fpls.2020.601009

Valdes-Abellan J., Pardo M.A., Tenza-Abril A.J., 2017. Observed precipitation trend changes in the western Mediterranean region. International Journal of Climatology 37, 1285–1296.

Velasco Amo M.D.P., Olivares-García C., Román-Écija M., Marco-Noales E., Navas-Cortés J.A., Landa del Castillo B.B., 2025. Modeling the accuracy of *Xylella fastidiosa* molecular diagnostic tests in naturally-infected almond tree samples. Plant Disease on line first. https://doi.org/10.1094/PDIS-12-24-2568-RE

Wells J.M., Raju B.C., Hung H.-Y., Weisburg W.G., Mandelco-Paul L., Brenner D.J., 1987. *Xylella fastidiosa* gen. nov., sp. nov: Gram-Negative, Xylem-Limited, Fastidious Plant Bacteria Related to Xanthomonas spp. International Journal of Systematic and Evolutionary Microbiology 37, 136–143. https://doi.org/10.1099/00207713-37-2-136

Funded by the European Union